

Journal of Petroleum and Gas Engineering

Volume 8 Number 10 December 2017

ISSN 2141-2677



*Academic
Journals*

ABOUT JPGE

Journal of Petroleum and Gas Engineering (JPGE) is an open access journal that provides rapid publication (monthly) of articles in all areas of the subject such as Petroleum geology, reservoir simulation, enhanced oil recovery, Subsurface analysis, Drilling Technology etc.

The Journal welcomes the submission of manuscripts that meet the general criteria of significance and scientific excellence. Papers will be published shortly after acceptance. All articles published in JPGE are peer-reviewed.

Journal of Petroleum and Gas Engineering is published monthly (one volume per year) by Academic Journals.

Contact Us

Editorial Office: jpe@academicjournals.org

Help Desk: helpdesk@academicjournals.org

Website: <http://www.academicjournals.org/journal/JPGE>

Submit manuscript online <http://ms.academicjournals.me/>

Editors

Dr. Chuanbo Shen

Department of Petroleum Geology,
Faculty of Earth Resources,
China University of Geosciences
Wuhan, Hubei 430074,
P. R. China.

Dr. Amir Hossein Jalili

Research project manager,
Gas Science Department,
Research Institute of Petroleum Industry (RIPI),
Tehran
Iran.

Dr. Salima Baraka-Lokmane

Senior Lecturer in Hydrogeology,
University of Brighton,
Cockcroft Building, Lewes Road,
Brighton BN2 4GJ,
UK.

Abouzar Mirzaei-Paiaman

Production Engineer
Department of petroleum engineering,
National Iranian South Oil Company (NISOC),
Iran.

Mobeen Fatemi

Department of Chemical and Petroleum
Engineering,
Sharif University of Technology,
Tehran,
Iran.

Prof. Yu Bo

Beijing Key Laboratory of Urban Oil and Gas
Distribution,
Technology Department of Oil and Gas Storage and
Transportation, China University of Petroleum –
Beijing
Beijing,
P. R. China, 102249.

Editorial Board

Dr. Haijian Shi

Kal Krishnan Consulting Services,
Inc., Oakland, CA

Dr. G Suresh Kumar

Petroleum Engineering Program
Department of Ocean Engineering
Indian Institute of Technology – Madras
Chennai 600 036
INDIA

Journal of Petroleum and Gas Engineering

Table of Contents: Volume 8 Number 10 December 2017

ARTICLES

- | | |
|---|------------|
| Downhole flow controllers in mitigating challenges of long reach horizontal wells: A practical outlook with case studies | 97 |
| Omar Jamal Chammout, Bisweswar Ghosh and Mohamad Yousef Alklich | |
| Analysis and field applications of water saturation models in shaly reservoirs | 111 |
| Shedid A. Shedid and Mohamed A. Saad | |

Review

Downhole flow controllers in mitigating challenges of long reach horizontal wells: A practical outlook with case studies

Omar Jamal Chammout, Bisweswar Ghosh and Mohamad Yousef Alklich*

Petroleum Engineering Department, Petroleum Institute, Abu Dhabi, United Arab Emirates.

Received 26 June, 2017; Accepted 1 September, 2017

Production and injection in long reach horizontal wells pose several challenges in production optimization, flow assurance and reservoir management. Horizontal wells are known to be superior to vertical wells in terms of productivity, however, they are also susceptible to early water and/or gas cut production due to the heel-toe effect and/or permeability contrasts. Uniform distribution of water injection into all zones can also be a challenge in case of high-permeability streaks and fractures. To negate some of the adverse reservoir properties and to control the flow profile of production and injection fluids, downhole flow control devices are increasingly in use and beneficial in regulating flow, improved overall reservoir sweep, improved productivity from the tail section of the well and reduced water coning or gas cusping. Wellbore hydraulics for a long reach well completed with downhole valves have great influence on the reservoir performance and recovery in the long run. This paper presents a discussion aimed at better understanding of the critical challenges that long reach horizontal wells are prone to in terms of completion, as well as the developments so-far that have been applied to capture the physics across the long horizontal section. Three case studies are also discussed with some details emphasizing practical experiences of such wells.

Key words: Downhole flow controllers, horizontal wells, inflow control devices (ICD), internal control valves (ICV), production enhancement.

INTRODUCTION

Application of horizontal drilling technology in oil field development and production operations has grown significantly over the past decade. It has been achieving commercial viability since late 1980's which encouraged horizontal drilling in various geographic regions and geologic settings. Achievable horizontal borehole length grew swiftly as drilling technologies advanced. Horizontal displacements nowadays have been extended over

20,000 ft. Completion and production techniques have also developed for the horizontal borehole environment at equal pace.

Numerous potential advantages are associated with horizontal wells namely, well productivity, sweep efficiency and delayed water and gas coning due to increased wellbore-reservoir contact area.

These can be summarized as follows (Salamy, 2005):

*Corresponding author. E-mail: malklich@gmail.com. Tel: +971 (50) 6158581.

- (1) Minimized unit development costs.
- (2) Minimized unit operating costs.
- (3) Minimized drawdown at a given flow rate.
- (4) Minimized water and gas breakthrough (in homogeneous reservoir).
- (5) Maximized long term performance.
- (6) Maximized production rate / PI.
- (7) Maximized sweep efficiency / reserves.

Despite numerous advantages of drilling those long Maximum Reservoir Contact (MRC) wells and multilaterals, they are associated with unprecedented challenges in the areas of drilling and completion, mostly due to the complex wellbore fluid dynamics resulting from the extra exposure with the reservoir (Salamy, 2005).

Production from conventional well is controlled at surface by manipulating the wellhead choke to control the production of gas and/or water in high GOR – WOR wells. This technique is no longer sufficient in MRC wells because having such a long contact between the wellbore and the reservoir does not drain the reservoir uniformly. In MRC wells, premature breakthrough of unwanted fluids (gas and/or water) occurs due to several reasons, some of which are listed and further discussed below.

- (1) Frictional pressure losses along the wellbore which is sensitive to the length of the wellbore, a phenomenon known as the heel-toe-effect.
- (2) Reservoir permeability heterogeneity due to the geological setting of the reservoir in the depositional environment.
- (3) Variation in the distance between the wellbore and the gas/water flood front due to factors such as an inclined wellbore or tilted flood front.
- (4) Variations in reservoir pressure due to penetration of several pressure regions of the reservoir.
- (5) Variation in encroachment of injected water and gas profile along the wellbore due to permeability heterogeneity and heel-toe effect in the injector wellbore.

The heel-toe-effect is defined by the difference in the specific inflow/outflow rates between different sections of the wellbore, particularly evident when comparing the near shoe section (the heel) and the near target depth section (TD – the toe). This phenomenon arises due to the frictional pressure drop along the wellbore which becomes more and more significant when its value approaches the threshold drawdown pressure. The heel-toe phenomenon is most evident in high permeability reservoirs producing at high fluid rates which in turn generate increasing significant frictional coefficient along the wellbore. To prevent or minimize this phenomenon in high permeability reservoirs, drilling a larger diameter hole or limiting to shorter laterals are technically feasible option, however this may not be economically feasible (Minulina et al., 2012).

The other three challenges (listed 2, 3, and 4 above) may possibly be mitigated (at least theoretically) through an optimized and accurate design of wellbore trajectory. Inadequate identification of the parameters during the time of designing the trajectory or even during actual drilling, will lead to improper designing of the completion for the drilled well (Raffin et al., 2007).

Production from horizontal wells imposes even greater challenges as they are vulnerable to various factors impacting production such as well cleanup and water coning or gas cusping (which are mainly caused by reservoir heterogeneity, depicted by permeability contrasts within the wellbore). On the other hand, water injectors are susceptible to an uneven flow profile, poor sweep efficiency and large amount of bypassed oil due to inability to achieve even distribution of water into all penetrated zones. These challenges are usually attributed to reservoir heterogeneity, permeability anisotropy, presence of fractures and/or faults and also the frictional losses causing unintentional thermal fracturing during water injection (Minulina et al., 2012). In long horizontal injection wells, even if permeability heterogeneity is less significant, the heel-toe effect caused by severe frictional pressure loss may flood the heel zone early in the injection period and cause early water breakthrough in the nearby producers, leaving behind large recoverable reserve in the toe section (Birchenko et al., 2010).

In highly heterogeneous and fractured reservoirs with openhole completion (completions with pre-drilled or slotted liners without packer segmentation are also considered “openhole completion” in this article), excessive flooding in high permeability streaks may be resulted, while lower permeability streaks may undertake little or no water. Therefore, the risk of non-uniform water injection and early water breakthrough in the adjacent production wells should be expected (Garcia et al., 2009).

The movement of reservoir fluids between injectors and producers in conventional completions are controlled by reservoir and fluid properties but also governed to a large degree by injection and production rates and profiles. Profound understanding of the reservoir topology, its geological setting and connectivity of various compartments, and the dynamic interactions between wells are critical for setting optimal field development plans and production strategies. Therefore, decisions concerning production and injection rates, well placement, and completion design are all affected by the outcomes of dynamic reservoir simulations during its lifespan (Garcia et al., 2009).

Proven and practical solutions to the above challenges when addressed collectively in well completion design are currently termed as smart completions, by which downhole inflows and outflows are controlled by various devices attached during well completion. The principle is to control or restrict the flow from the annulus into the production string or vice versa (Daneshy et al., 2010).

The distribution and setting of the restrictions are designed carefully to improve the areal and vertical sweep efficiency by establishing a stable flood front around the wellbore and hence preventing unwanted fluid breakthrough (Ouyang, 2009). Two major types of smart completion devices are as follows:

- (1) Internal Control Valves (ICV)
- (2) Inflow Control Devices

To design an effective smart completion, it is essential to perform dynamic reservoir simulation, which demonstrate the potential benefits of utilizing smart completions in both injectors and producers, especially in highly heterogeneous reservoirs. Employing a smart completion design to balance out the influx of a producer well or the out flux of an injector well, that is, attempting to create a uniform and stable flood front in the reservoir, provides tangible benefits in terms of delayed water breakthrough, increased production rate and optimized injection rate and hence increased recovery (Aadnoy and Hareland, 2009; Gao et al., 2007).

However, installing smart completion in a long horizontal well may incur a huge additional completion cost and may impact profitability of the project. Instead, a simpler completion solution such as slotted liner (with or without zonal isolation packer) may be an attractive solution in profiling produced oil or injection water in a relatively homogenous reservoir. Another solution which could be more attractive compared to the simple slotted liners in terms of technical and cost effectiveness is the engineered slotted liner or the Limited-Entry Liner (LEL). The LEL can compensate the variation in reservoir permeability across the long horizontal section by varying both the density and the size of the openings or slots in the liner (Burtsev et al., 2006; Chow et al., 2009).

COMMON CHALLENGES IN HORIZONTAL PRODUCTION WELLS

As mentioned previously, horizontal wells do enhance wellbore-reservoir contact, oil production, and reduce the number of wells needed to develop a certain field compared to vertical wells. However, there are several associated challenges that must be addressed prior to the design and development of a field with horizontal wells (Augustine, 2002). These challenges are discussed next.

Coning

Most reservoirs have an underlying water zone and/or an overlying gas cap. When production is started, a pressure sink occurs along the wellbore. The fluids flow towards the point in the wellbore where the drawdown is maximum.

In some cases, coning in horizontal wells could be expedited because of the heel-toe effect and the variable permeability distribution along the well bore (Richardson et al., 1987).

Heel-Toe effect

Between the first point of contact of the wellbore with the reservoir (heel) and the end of the wellbore (toe), there will be a frictional pressure drop along the horizontal section of the wellbore. For long horizontal wells with high flow rates, frictional and acceleration effects can cause significant pressure drop and therefore reduce the effective wellbore conductivity. This implies that the fluid influx can be greater at the heel and gradually lower towards the toe as fluids experience frictional pressure drop as they move from the toe to the heel (Birchenko et al., 2010). In homogenous reservoirs, water and gas cone towards the heel is frequent, resulting in premature water/gas breakthrough (Figure 1 Left). One solution of this problem is to introduce flow restriction in accordance to the pressure drop profile, using inflow controllers. When Inflow Control Devices (ICD) and zonal isolation packers are in place, the fluid influx will be restricted at the heel, thus flow from toe side will be eased (Al Marzouqi et al., 2010). Oil flow towards the wellbore would be more uniform, thus delaying water breakthrough as depicted in Figure 1 right.

Variable permeability and pressure distribution

The rock matrix along the wellbore varies in permeability consequently leading to an uneven inflow, giving an effect similar to pressure contrasts. The fluids seek the path of least resistance and therefore flow through the high permeable zones and fractures, resulting in water or gas breakthrough at these points along the wellbore. As clearly shown in Figure 2, the ICD integrated completion is used to equalize the pressure drop between the different sections, ultimately balancing the fluid influx.

Premature water/gas breakthrough

Due to coning and near wellbore formation fracturing and damage, water and gas may enter the well at an earlier stage of production than anticipated. This results in less oil production, and more amount of the unwanted fluids, leading to a higher processing costs and system bottlenecking. This is to be considered during the completion design stage as it may influence the produced volume of oil. Proper flow controller integration during completion design can delay the water and gas from entering the well, effectively extending the lifespan of the well. When water or gas eventually enters the well, the higher mobility fluids choke the inflow, according to

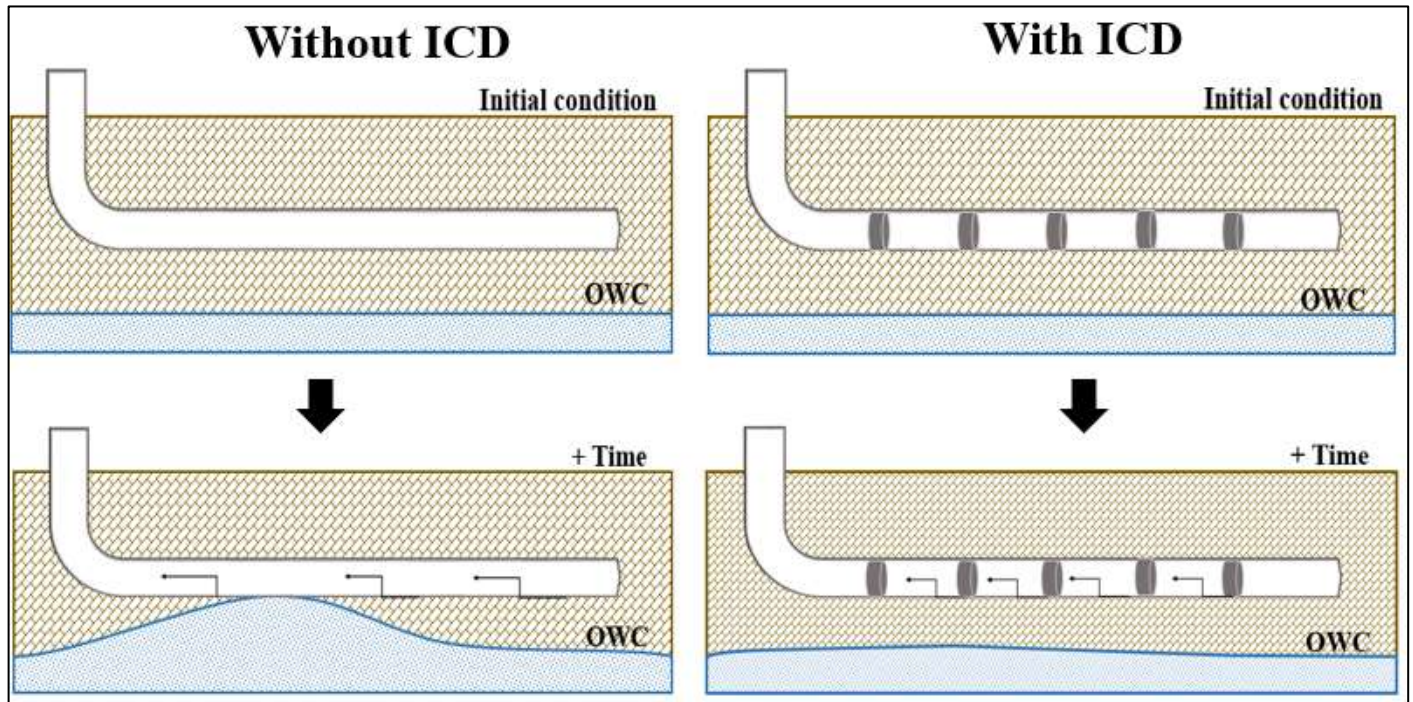


Figure 1. Combined effect of Coning and Heel-toe effect in homogeneous reservoir and mitigation using ICD.
Source: Jokela (2008).

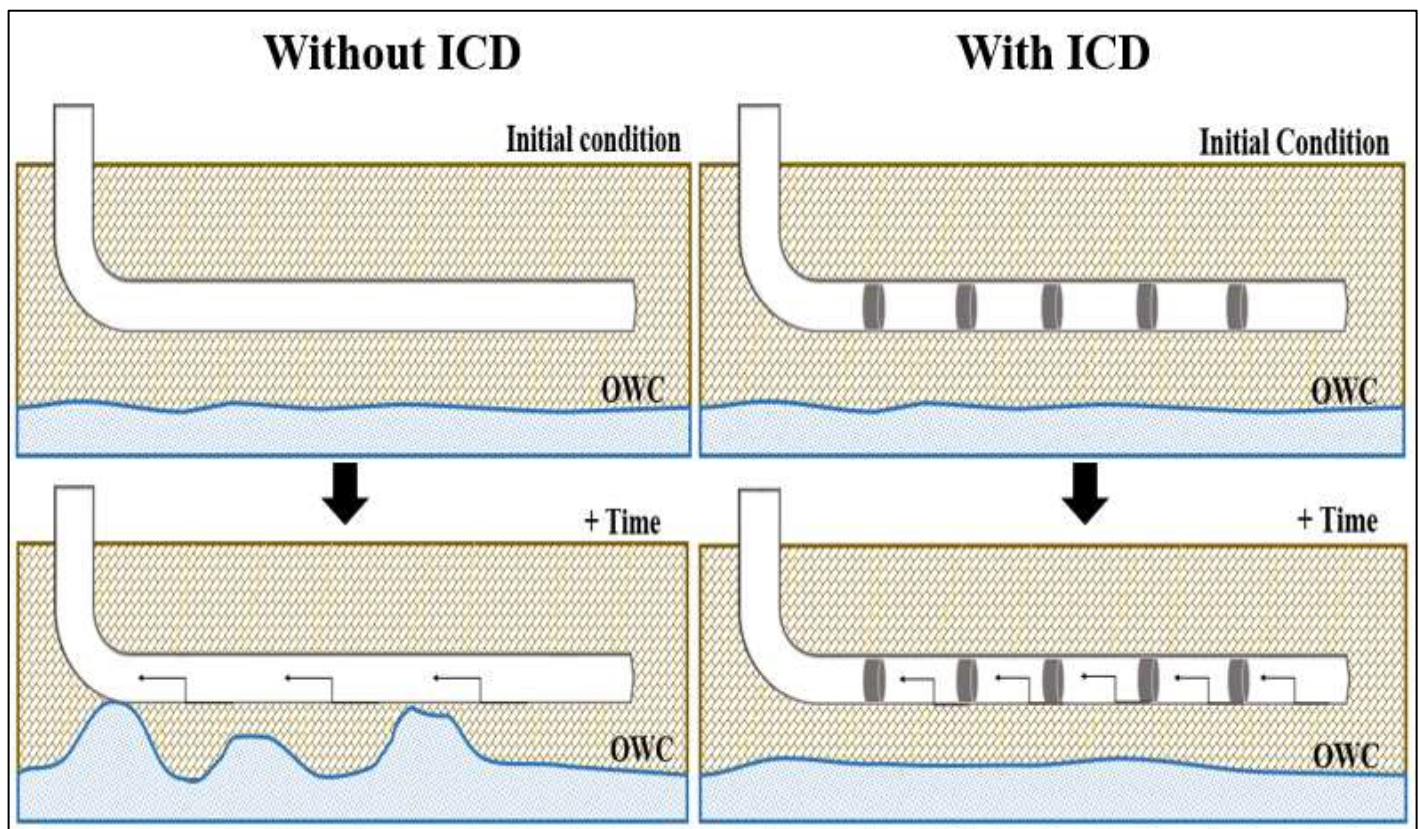


Figure 2. Mitigating effect of ICD in heterogeneous reservoir.
Source: Jokela (2008).

pressure drop in Bernoulli's equation (Al-Khelaiwi and Davies, 2007):

$$\Delta P = \rho \cdot \frac{v^2}{2}, \quad v = \frac{q}{A} \quad (1)$$

where ΔP is the pressure drop, ρ is the density of the fluid, v is the fluid flow speed, q is the flow rate and A is the area of the cross-section of the horizontal hole.

Poor wellbore clean-up

Long reach horizontal wells are prone to increased levels of formation damage (more positive skin factor) due to the increased exposure of the formation to the drilling and completion fluids under overbalance conditions. The result of formation damage is basically an additional pressure drop resulting in decreased productivity as illustrated in the equations below.

$$\Delta P_{DD} = \Delta P_{ideal} + \Delta P_{skin} \quad (2)$$

$$J = \frac{q}{\Delta P_{DD}} = \frac{q}{\Delta P_{ideal} + \Delta P_{skin}} \quad (3)$$

where ΔP_{DD} is the total pressure drawdown, ΔP_{ideal} is the pressure drawdown without formation damage, ΔP_{skin} is the additional pressure drawdown due to skin, J is the productivity index and q is the flow rate.

The residual filter cake after drilling a well requires optimum and uniform well flow to pop up and flow back the residual cakes. This process is usually termed as well clean-up. Due to the non-uniform influx in horizontal wells, zones that experience low productivity finds difficulty in removing the filter cakes, resulting in higher skin and poor well clean-up. A common way to do wellbore clean-up is by increasing drawdown. However, the extended length of the horizontal well imposes a variation in the drawdown along the horizontal section, making it impossible to ensure that there is sufficiently enough high drawdown to remove the filter cake and reduce the formation damage, particularly in the toe area of the hole (Al-Khelaiwi et al., 2009). Additionally, pushing the drawdown into high values may not always be gainful; as this may lead to wellbore collapse, accelerated water and/or gas coning and encouraging sand production (Maclachlan and Harper, 2016).

Achieving an even inflow profile through the equalizing effect of ICD is beneficial to efficiently clean the long horizontal wells; particularly for those horizontal wells with large variation in reservoir parameters and where there is a significant heel-toe effect. Sequential opening and closing of valves allows imposing higher drawdown on one zone after another, providing better clean-up than conventional completion and resulting in better near

wellbore pressure profile and higher well productivity as illustrated in Figure 3 (Jones et al., 2009; Raffn et al., 2008).

COMMON CHALLENGES IN HORIZONTAL INJECTION WELLS

Non uniform outflow

At formations with heterogeneous/stratified geology, the injected water seeks the path of least resistance in both the near wellbore and throughout the sweep zones. This results into non-uniform sweep and lower recoverable reserves (Chen et al., 2011). In homogenous reservoirs, the injection pressure is highest at the heel of the wellbore; the outflow of water will be concentrated at the heel while reduced amounts reach the toe. Figure 4 illustrates the heel-toe effect with a garden hose analogy which has a set of openings in it.

ICD integrated completions can regulate the high intake zones. While the low permeable zones will have larger openings so that a more uniform flow across the whole wellbore can be achieved. This way, the heel-toe effect, the permeability contrasts effect, and fractures effect can be mitigated (Neylon et al., 2009). Also, applying an ICD integrated completion in an injector well results in an even water distribution throughout the wellbore, resulting in enhanced sweep effect as shown in Figure 5.

Fracturing

Water injection can impose formation damage and induce fractures in the near wellbore region. The most common causes are thermal induced stress changes, changes in pore pressure and injection pressure build-ups due to plugging. These fractures can have very high permeability causing the injected water to flow in larger quantities into the fractures. After some time, the fractures grow wider because of erosion effects and pressure differences. The water will then flow along fractures and high permeability zones even more, reaching the producer earlier than anticipated (Gadde et al., 2001). Using ICDs in addition to zonal isolation can reduce the risk of thermal fracturing, by regulating the flow from high intake to low intake area.

Early water breakthrough

In the presence of the naturally occurring fractures, and high permeability streaks, the water outflow will be focused on these sections, and ultimately reach the producer prematurely. Zones with lower permeability will experience a reduced sweep or none at all. In addition to the reduced overall production and the bypass of potential recoverable oil reserves, the increased amount

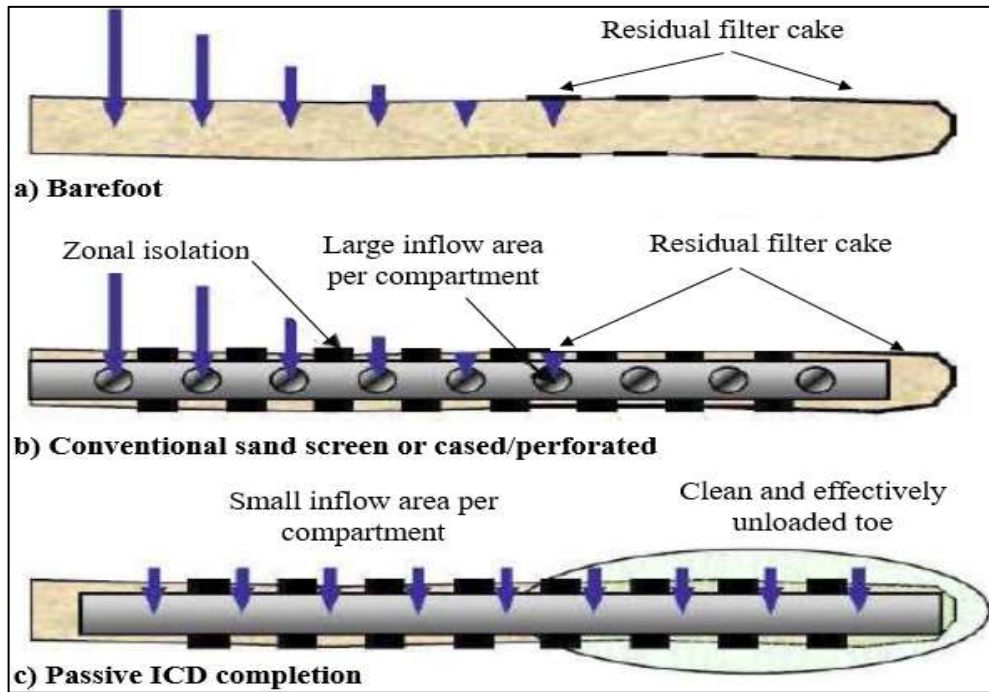


Figure 3. Well cleanup properties for barefoot, sand screen and ICD Completion, respectively. Source: Raffin et al. (2007).

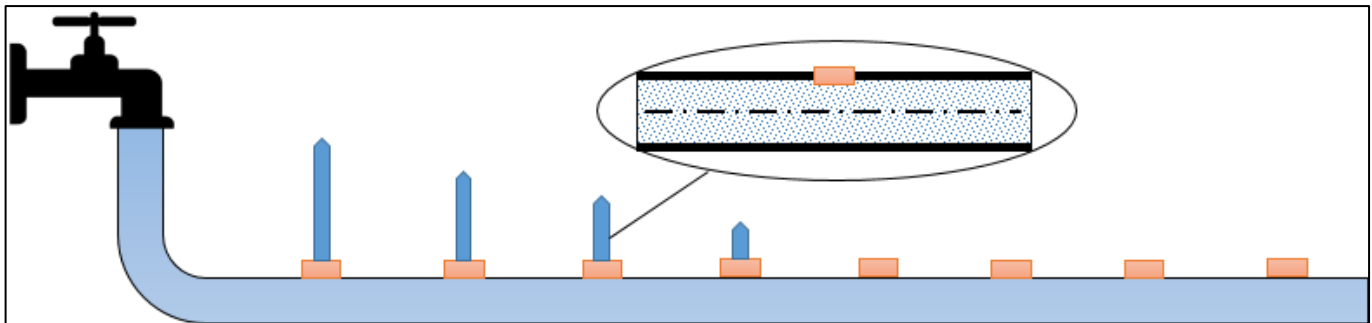


Figure 4. The heel-toe effect illustrated with a garden hose figure with a set number of openings (open hole case). Source: Jokela (2008).

of produced water will have higher processing cost and therefore impact short and long term profit generation. Water flow profiling with the help of inflow controllers are designed to mitigate this issue by enabling a more even influx along the wellbore (Augustine et al., 2006; Youl, 2011).

MECHANICAL CONFORMANCE TECHNOLOGY

A conformance technology is a method of managing the profile and controlling the volume of unwanted water or gas production. Before 1990s, the common practice was the use of chemical treatments such as relative

permeability modifiers or polymer gels, known as chemical conformance modification (Thornton et al., 2010). In the 1990s, the demand for the mechanical conformance technologies arose after the development of the first inflow control valve (ICD); as they proved that their CAPEX and deployment overhead is relatively small compared to their advantages. ICDs were installed in thousands of wells worldwide over the last decade and are considered a mature well-completion technology. They mainly work to equalize the inflow along the horizontal wells by imposing additional pressure drop in the more flow contributing zones and consequently reducing the drawdown within the interval (Smith et al., 2016); as explained by the following equations.

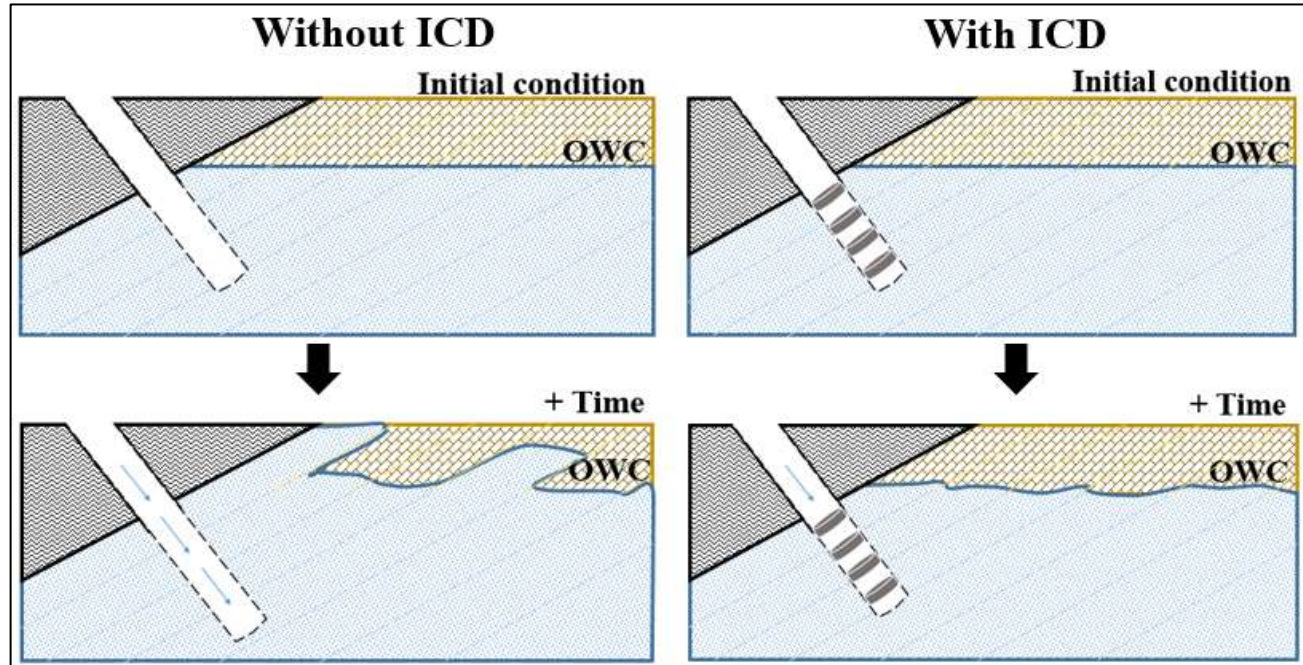


Figure 5. Injection profile in heterogeneous reservoir with and without an ICD solution.
Source: Neylon et al. (2009).

$$\Delta P_{ICD} = P_{nw} - P_{wf} \quad (4)$$

$$\Delta P_{DD} = P_r - P_{nw} \quad (5)$$

where ΔP_{ICD} is the pressure drop across the ICD, P_{nw} is the flowing well pressure, P_{wf} is the flowing bottomhole pressure, ΔP_{DD} is the total drawdown pressure and P_r is the reservoir pressure.

The mechanical conformance technologies were fast developed both in technology and number of deployment in proportion to the huge increase in the number of long horizontal wells drilled and completed (Lauritzen et al., 2011). The long reach wells access a much bigger portion of the reservoir than the vertical and deviated wells, and thus, are exposed to higher permeability heterogeneity. The advanced completion equipment and downhole devices are supposed to maintain a uniform production profile along the horizontal section, and manage the breakthrough of the unwanted fluids (Shi et al., 2016). The completion strategies includes, but are not limited to, open hole, cased hole, slotted liners, downhole inflow regulators and valves, sand screens, and engineered slotted liners.

There are two main aspects in an effective mechanical conformance technology (Thornton et al., 2010):

- (1) Proper selection of the downhole control device
- (2) Proper placement of the selected flow control device

There exist so many types and models of the downhole control devices, and the selection is rather not so complicated. The main challenge however is the proper placement of the control devices and the segmentation of the horizontal wellbore. This is the subject of next discussed.

Wellbore simulation

A well is represented as node (sink or source) in a conventional reservoir simulator. In the reservoir simulator, the well model is used to correlate block pressure, production rate, and bottomhole pressure. A skin factor is used to count for the other completion designs. However, a simple skin factor is not enough to represent the wellbore hydraulics and how it changes over time. Unfortunately, at earlier times, there was no method to properly place the downhole tools and to accurately diagnose the conformance challenge related to well completion (Wang et al., 2008; Edmonstone et al., 2015).

Service providers and operating companies critically demand to have a software that simulates wellbore hydraulics in order to count for the pressure drops across the variable completion components along the horizontal drain (Grubert et al., 2009). Some vendors create a steady state simulator that models multi-phase flow across the wellbore region.

These software calculate overall production

performance, inflow profile, pressure profile, and flow rates in tubing and annulus. The static or the steady state simulator requires reservoir input data such as well boundary conditions, reservoir pressure, phase mobility, and solubility factors. The steady state simulator works to enhance the design of the completion and the selection of the downhole devices. Hence, since it is a static simulator, the wellbore hydraulics simulation is done at a single time step (Carvajal et al., 2013; Awad et al., 2015).

Coupling dynamic and static simulators

The static or steady state simulator can be used to create a detailed model of the wellbore completion but only has a simplistic representation of the reservoir. Therefore, by coupling steady state and the numerical simulators, we can leverage the capabilities of each software to make more accurate models. A coupled model dynamically captures the coupled effects of wellbore hydraulics and reservoir simulation improving the accuracy of the simulation. Some of the reported advantages of coupling static and dynamic modeling include (Vasper and Gurses, 2013):

- (1) The use of properties distribution such as permeability and water saturation becomes more accurate and therefore contributes to a more accurate fluid flow predictions.
- (2) Compartment sizes, packer locations, predicted pressure and flow profiles can be further optimized.
- (3) Unwanted fluids breakthrough time can be computed.
- (4) Considers other producers/injectors and their cumulative production/injection effect.

Preparing the coupled simulation model is a significant undertaking that requires additional effort than that required for using any of the standalone softwares. Simulation runtime also increases significantly. While an individual static model takes seconds to converge, the steady state simulator requires additional time when coupled. The coupled model is also less stable requiring more pipe flow iterations and shorter time steps (Wang et al., 2008). Due to this increased amount of overhead, coupling is only undertaken when the increase in accuracy justifies the additional cost.

Therefore, the most common uses of such coupled models are in the following situations (Jackson et al., 2012):

- 1) When the completion has a direct impact on reservoir performance and overall field recovery (e.g. annular flow impacts on performance).
- 2) When complex completions such as ICDs are used to improve reservoir recovery performance.

The coupled simulator is used specifically to optimize the design of the completion string and the downhole equipment as per the following (Thornton et al., 2010):

- (1) Calculate the effect of the downhole device on the overall reservoir performance forecast.
- (2) Obtain better understanding of the reservoir mechanics.
- (3) Decrease operational risks and costs.
- (4) Enhance the design of the completion and consequently maximizing NPV to the operator.
- (5) Study placement strategy for the downhole barriers and packers.
- (6) Assist in material and equipment selection and therefore save OPEX on possible future well intervention operations such as workover or stimulation.

FIELD APPLICATIONS – CASE STUDIES

The coupled simulation is relatively an up-to-date practice. There are very few field examples that are published in the literature. The following are some field applications of the coupled modeling methodology, emphasizing the practical experiences of horizontal wells with smart completions.

Case study 1

A study has been conducted in ADMA-OPCO in order to assess the efficiency of implementing inflow control devices in improving the recovery from a highly heterogeneous under-saturated carbonate reservoir. This study was part of a major development plan where the company was attempting to implement smart completion technologies, ICD being one of them. A sector model was extracted from the full field model so that simulations can be run and then evaluations can be made for the different sector models (Marir et al., 2011).

As mentioned earlier, implementing ICD integrated completion designs in oil producers or water injectors generally delivers considerable enhancement in reservoir control by balancing the fluid flow front and achieving a uniform flow profile. There are however certain challenges where the demand for utilizing ICDs arises. Those challenges are as follows:

- (1) Non-uniform drawdown distribution, known as heel-toe effect.
- (2) Permeability contrasts.
- (3) Mobility contrasts.
- (4) Variation in reservoir pressure.

Based on the listed challenges, several completion cases were put in place for investigation. The cases that were investigated in this research are the following:

Case 1: Open hole oil producer (as reference case) + Open hole water injector.

Case 2: Cased hole oil producer with ICDs along the total drain + Open hole water injector.

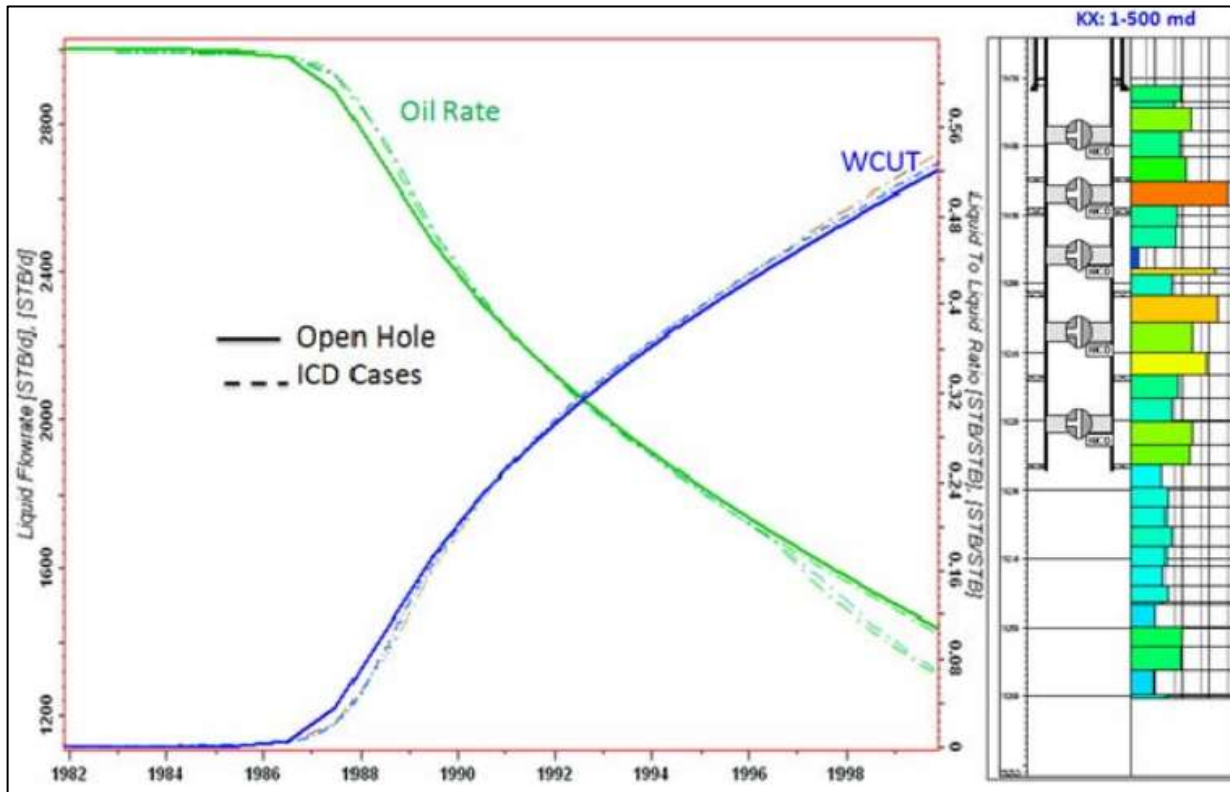


Figure 6. Well performance with and without ICDs in Reservoir A.
Source: Marir et al. (2011).

Case 3: Cased hole oil producer with ICDs in the upper zone and open hole in the lower zone + Open hole water injector.

Case 4: Cased hole oil producer with ICDs + Water injector + High permeability streak crossing the producer & the injector.

Different design parameters were considered, such as the number of ICDs, number of nozzles, nozzle sizes, and number of compartments (swellable packers).

The results of this study showed that implementing ICD integrated completions led to uniform production distribution along the horizontal drain. However, it did not show significant improvement in the recovery of oil (Figure 6).

This unexpected outcome was investigated. It is believed that the relative permeability data used in the simulation are limited and may present weakness in describing the fluid flow in different rock type. The reservoir consists of different units which make the use of ICDs viable, while the sector model used in this study acts as a tank, so the fluid that was restricted to flow in a certain compartment will be basically produced from another compartment. This conclusion is very important and advises a careful selection of the sector model that should be used in this type of work.

Case study 2

Conventional simulation modeling generally neglects the pressure distribution within the wellbore. It is assumed that the fluid inflow across each completed interval is directly proportional to the length of the wellbore and the permeability of the reservoir cell. Vertical lift performance curves are used to estimate the tubing head pressure. In reality, there is a friction pressure drop which has a significant impact on the pressure distribution along the wellbore. There will be a higher inflow at the heel of the well since fluids there are subject to less friction pressure. Conventional simulation modeling does not count for such pressure variation in the wellbore (Minulina et al., 2012).

Wellbore modeling tools allow simulation of multilateral wells considering wellbore friction, and downhole choking devices. This is done by providing a thorough description of fluid flow in the wellbore. Coupling the wellbore model and the reservoir model gives a precise tool for designing and planning multilateral and horizontal wells.

The wellbore is subdivided into multiple segments in a process that is known as multi-segmentation. Each segment or compartment is represented by a node and describes flow path to its parent segment node. Modeling is done with nozzles, chokes, and other smart completion devices. Different keywords are used for modeling the

wellbore segments and their connection to the reservoir nodes. This allows the engineer to precisely describe the completion characteristics that control the flow along, across, and within the wellbore. Hereby, it is important to mention that detailed information about the completion components and their characteristics and functionality is of high importance to simulate near wellbore flow behavior with reasonable accuracy. It also allows comparison between different completion designs with different completion components. The following shows the steps of designing an ICD completion (Minulina et al., 2012):

- (1) "Use the reservoir simulation model to forecast the production profile and water saturation throughout the life of the field. Extract a permeability profile along the lateral length of the well from the reservoir model grid."
- (2) "Use a software such as "NeTool™" to design an ICD configuration that delays water or gas breakthrough and promotes oil production for the life of the well. Consider several options and determine the best configuration."
- (3) "Confirm initial model using real time logs during drilling."
- (4) "After reaching TD, refine the ICD design using real time log and a quick petrophysical evaluation for fluid saturation and permeability."
- (5) Use the multi-segment option and the detailed wellbore modeling to re-run the reservoir simulation. This is to double check the initial design and make necessary changes."
- (6) "Observe sensitivities to heterogeneity, behind pipe channeling, and well spacing."
- (7) "The final design should be reviewed with the well engineer for operational considerations before submitting to the completion engineer and the company man on the rig to start operations."

The concerned field, where the ICD completion is designed and implemented, is located offshore of Nigeria. It is considered as an excellent reservoir in terms of high porosity and permeability, but suffers from high permeability contrast (500 mD -15 D). Some of the flow intervals have very high permeability and are connected to the aquifer. Other sections have lower permeabilities and restricted lateral extent.

Static and dynamic simulations were run in order to come up with a unique completion design that is suitable for this field. One of the primary objectives of having such unique completion design is to block the rapid water encroachment from the highly permeable intervals. The following completion designs were considered during the modeling phase:

- (1) Cased hole perforations.
- (2) Slotted liners.
- (3) Wire wrapped screen.
- (4) Inflow control devices.

All producers were completed with ICD integrated

completions. The first two injectors were completed with wire-wrapped screens and blank pup-joints. The remaining injectors were completed using nozzle type ICD integrated completions. A producer and an injector pair was used as an example to study the effects of implanting ICDs in the wells. Three different scenarios were considered and compared. Those scenarios were the following:

- (1) Standard completion screens for both the producer and the injector.
- (2) ICD completion for the producer and standard screen for the injector.
- (3) ICD completions for both the producer and the injector.

Simulation results show that the ICD integrated completion for the producer only had a slightly higher recovery when compared to the wrapped screen completion. However, the scenario which had ICD completion for both the producer and the injector had a noticeable improvement in the recovery when compared to the of ICD completion for the producer only scenario. In addition, scenario 3 showed a better improvement in delaying water production. Figure 7 clearly demonstrates these results (Minulina et al., 2012).

The static simulator can show precisely how much the ICDs would influence the production for the inserted saturation data in the simulator. However, the timing of those saturations that was predetermined by the dynamic simulator was not accurate. This was because the ICDs would delay the breakthrough of the water and/or gas, and thus the saturation distribution would be different. In order to obtain more accurate results, the dynamic simulator was used in parallel with the static simulator.

Another important observation is that LWD logs that were obtained while drilling could be used to fine tune saturation and permeability data. Simulation could then be re-run and final adjustments be made on the completion design using the real time data.

For the injectors, simulations showed that ICD integrated completions gave a uniform and evenly distributed water front, while the wrapped screen design had preferential flow at the heel of the well. Behind pipe flow is an issue for the injectors because water would take the easiest flow path and having the ICDs in the completion would become useless. To solve this, there should be some isolation between the different ICD compartments. In consolidated formations such as carbonates, this can be done by implementing isolation devices such as swellable packers. In soft formations such as sandstones, this can be simply resolved by pre-producing the injectors in order to collapse the annulus and minimize behind pipe isolation.

Case study 3

This case study presents a conformance design on a

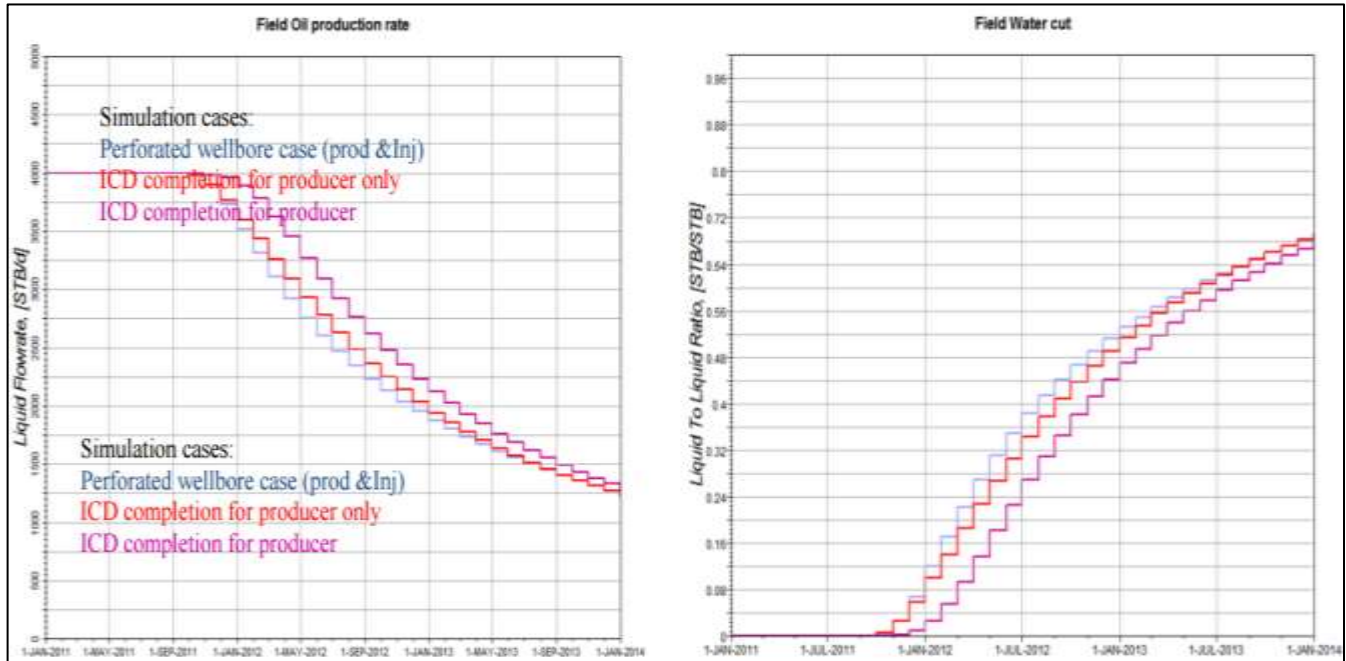


Figure 7. Field performance profiles, oil production (Minulina et al., 2012).

deviated well. The main concern in this well was the excessive water production from strong active aquifer. Huge quantity of produced water had to be re-injected into the reservoir though it was not necessary for pressure maintenance point of view. Figure 8 shows the production history of the first well in the study. The dots represent the actual production while the connected lines represent the history match resulted from the simulator (Thornton et al., 2010).

The well was planned to be completed with an ICD integrated completion in order to reduce the water cut and increase the produced oil. It can be observed from Figure 8 that there is a good match between the simulated and actual production. This gave extra confidence to go ahead and use the model to design an optimum ICD integrated completion.

The coupled simulator was used to study the fluid saturation changes in the reservoir. This enabled the reservoir and completion engineers to optimize the placement of ICDs and swellable packers in the wellbore.

Figures 9 and 10 show the oil and water production rates respectively for the base scenario and the ICD completion scenario. It is clearly shown in the figures that the ICD integrated completion enhanced the oil production and reduced the production of water.

CONCLUSION

The importance of this review stems from the fact that many future wells could benefit from the practices

mentioned here. Challenges, mitigation practices, field applications and wellbore simulation are subjects that were comprehended in this paper. A summary of the main highlights can be listed as below:

- (1) The demand for utilizing ICDs have been arising over the past decades to overcome certain critical challenges associated with production/injection in long reach horizontal wells. These include, but not limited to, water coning, heel-toe effect and permeability and mobility contrasts.
- (2) There are significant advantages in coupling the dynamic simulator with the static or steady state simulator. The coupled model provides detailed information on the annulus and tubing flow taking into account the effect of the downhole completion tools i.e. it operates by integrating wellbore nodal analysis into reservoir simulation to reflect the impact of the wellbore hydraulics on the reservoir flow and recovery in the short and long term.
- (3) The field cases presented in this paper shows the positive impacts of implementing the ICDs designs and coupled modeling on both history matching and reservoir production performance prediction. They also emphasized that the coupled modeling helps in material and equipment selection and therefore save OPEX on possible future intervention operations.
- (4) Future opportunities to develop smart completions and their simulators further are there in terms of determining the operating envelope containing the range of parameters suitable for downhole controllers.

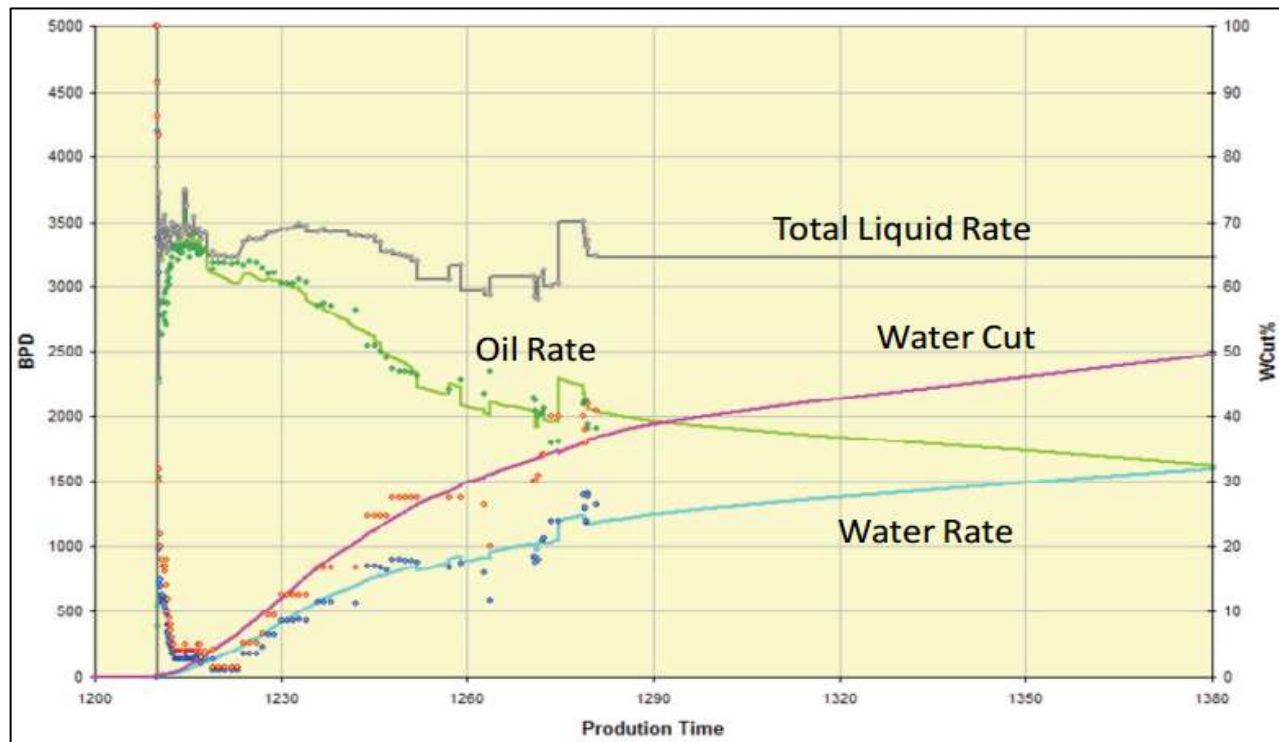


Figure 8. Production and simulator history match.
Source: Thornton et al. (2010).

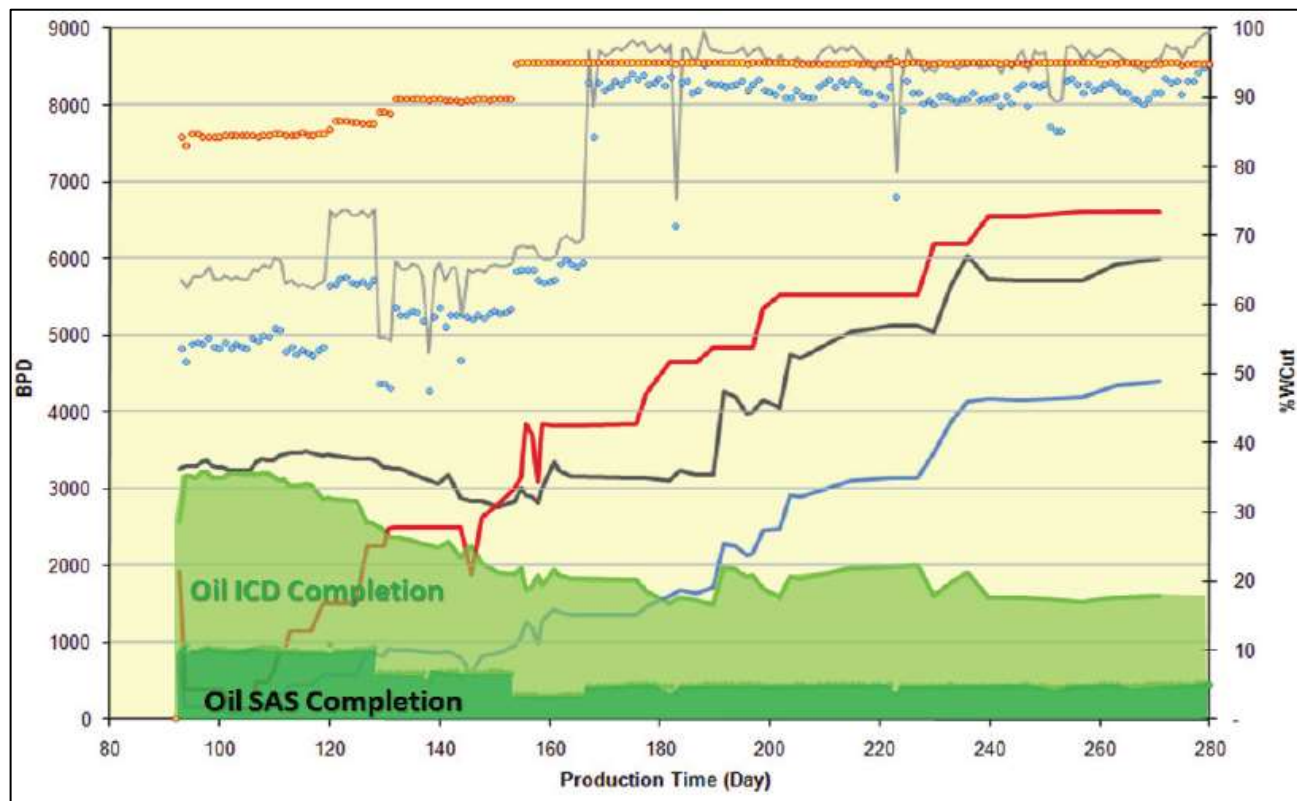


Figure 9. Oil production comparison between standalone screen (SAS) completion and ICD completion.
Source: Thornton et al. (2010).

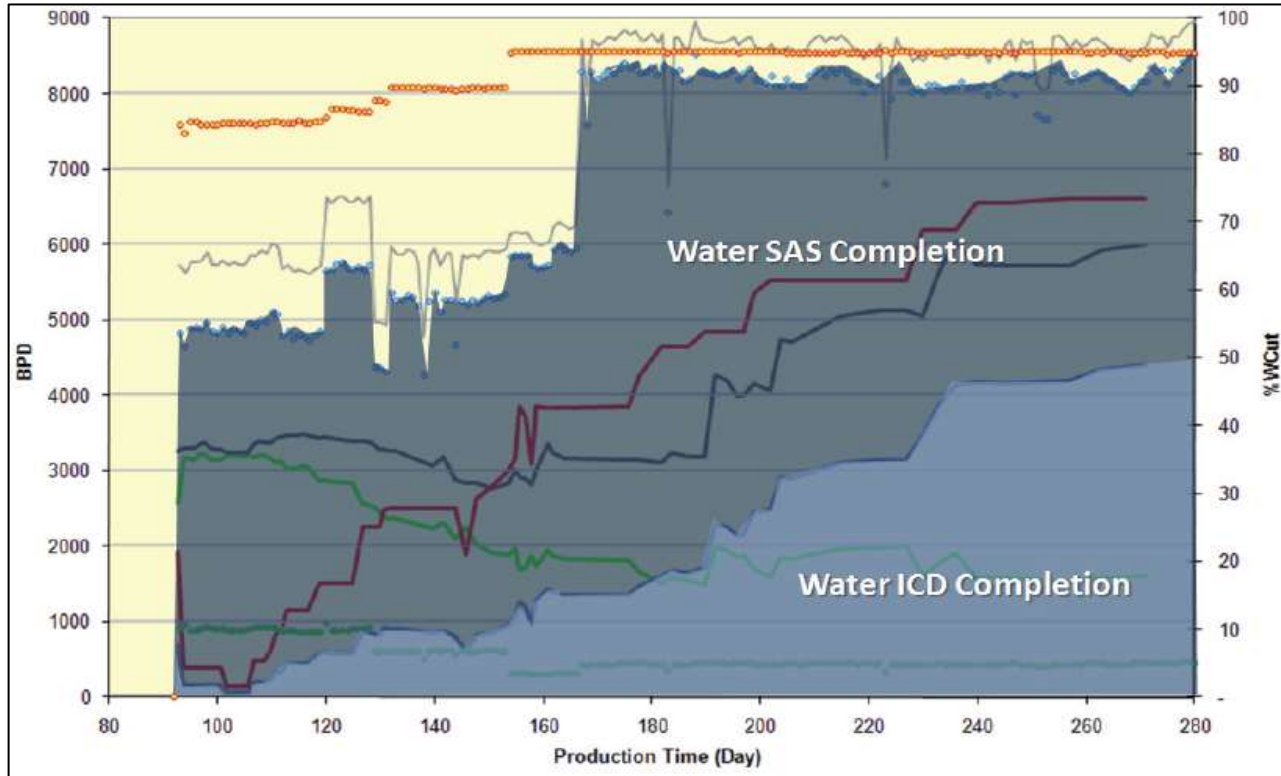


Figure 10. 1Water production comparison between standalone screen completion and ICD completion. Source: Thornton et al. (2010).

NOMENCLATURE

A , Cross-sectional area of the horizontal hole; ΔP , Pressure drop; ΔP_{DD} , Total pressure drawdown; ΔP_{ICD} , Pressure drop across the ICD; ΔP_{ideal} , Pressure drawdown without formation damage; ΔP_{skin} , Additional pressure drawdown due to skin; J , Productivity index; P_{nw} , Flowing well pressure; P_r , Reservoir pressure; P_{wf} , Flowing bottomhole pressure; ρ , Density of the fluid; q , Fluid flow rate; v , Fluid flow speed.

CONFLICT OF INTERESTS

The authors have not declared any conflict of interests.

REFERENCES

- Aadnoy B, Hareland G (2009). Analysis of Inflow Control Devices. Offshore Europe, Aberdeen, United Kingdom, 8-11 September. SPE-122824-MS.
- Al-Khelaiwi F, Davies D (2007). Inflow Control Devices: Application and Value Quantification of a Developing Technology. SPE International Oil Conference and Exhibition, Veracruz, Mexico, 27-30 June. SPE-108700-MS.
- Al-Khelaiwi F, Muradov K, Davies D, Olowolu D (2009). Advanced Well Flow Control Technologies can Improve Well Clean-up. 8th European Formation Damage Conference, Scheveningen, The Netherlands. 27-29 May. SPE-122267-MS.
- Al-Marzouqi A, Helmy H, Keshka A, Elasmr M, Shafia S (2010). Wellbore Segmentation Using Inflow Control Devices: Design & Optimization Process. Abu Dhabi International Petroleum Exhibition and Conference, Abu Dhabi, United Arab Emirates, 1-4 November. SPE-137992-MS.
- Augustine J (2002). An investigation of the economic benefit of Inflow Control Devices on Horizontal Well Completions Using a Reservoir-Wellbore Coupled Model. European Petroleum Conference, Aberdeen, United Kingdom, 29-31 October. SPE 78293-MS.
- Augustine J, McIntyre A, Adam, R, Laidlaw D (2006). Increasing Oil Recovery by Preventing Early Water and Gas Breakthrough in a West Brae Horizontal Well: A Case History. SPE/DOE Symposium on Improved Oil Recovery, Tulsa, Oklahoma, USA, 22-26 April. SPE-99718-MS.
- Awad MO, Al Ajmi MF, Safar A, Rajagopalan V (2015). Advanced ICD Application Alleviating Well Intervention Challenges. SPE Kuwait Oil and Gas Show and Conference, Mishref, Kuwait, 11-14 October. SPE-175204-MS.
- Birchenko V, Muradov K, Davies D (2010). Reduction of the horizontal well's heel-toe effect with inflow control devices. J. Pet. Sci. Eng. 75:244-250.
- Burtsev A, Ascanio F, Mollinger A, Kuvshinov B, De Rouffignac E (2006). Limited Entry Perforations in HVO Recovery: Injection And Production In Horizontal Wells. SPE Russian Oil and Gas Technical Conference and Exhibition, Moscow, Russia, 3-6 October. SPE-102656-MS.
- Carvajal G, Saldierna N, Querales M, Thornton K, Loaiza J (2013). Coupling Reservoir and Well Completion Simulators for Intelligent Multi-Lateral Wells: Part 1. EAGE Annual Conference & Exhibition incorporating SPE Europec, London, United Kingdom, 10-13 June. SPE-164815-MS.

- Chen J, Alfred D, Shang B, Hamman J (2011). Physics-Based Permeability Modeling. SPWLA 52nd Annual Logging Symposium, Colorado Springs, Colorado, USA, 14-18 May. SPWLA-2011-TT.
- Chow J, Blount C, Hilleary N (2009). Annular Isolation of Horizontal Slotted Liners with Chemical External-Casing Packers. SPE/ICoTA Coiled Tubing & Well Intervention Conference and Exhibition, the Woodlands, Texas, 31 March-1 April. SPE-121643-MS.
- Daneshy A, Guo B, Krasnov V, Zimin S (2010). ICD Design: Revisiting Objectives and Techniques. SPE Asia Pacific Oil and Gas Conference and Exhibition, Brisbane, Queensland, Australia, 18-20 October. SPE-133234-MS.
- Edmonstone G, Jackson A, Kofoed C, Shuchart C, Troshko A (2015). Acid Systems and ICD Design Considerations For Stimulation. Abu Dhabi International Petroleum Exhibition and Conference, Abu Dhabi, UAE, 9-12 November. SPE-177595-MS.
- Garcia L, Coronado M, Russel R, Garcia G, Peterson F (2009). The First Passive Inflow Control Device That Maximizes Productivity During Every Phase of a Well's Life. International Petroleum Technology Conference, Doha, Qatar, 7-9 December. IPTC-13863-MS.
- Gao C, Rajeswaran T, Nakagawa E (2007). A literature review on smart well Technology. SPE Production and Operations Symposium, Oklahoma City, Oklahoma, U.S.A, 31 March-3 April. SPE-106011-MS.
- Grubert M, Wan J, Ghai S, Livescu S, Brown W, Long T (2009). Coupled Completion and Reservoir Simulation Technology for Well Performance Optimization. SPE Annual Technical Conference and Exhibition, New Orleans, USA, 4-7 October. SPE-125521-MS.
- Jackson A, Al Azizi B, Kofoed C, Shuchart C, Keller, Sau S, Grubert M, Phi M (2012). Completion and Stimulation Methodology for Long Horizontal Wells in Lower Permeability Carbonate Reservoirs. Abu Dhabi International Petroleum Exhibition and Conference, Abu Dhabi, UAE, 11-14 November. SPE-161527-MS.
- Jokela T (2008). Significance of Inflow Control Device (ICD) Technology in Horizontal Sand Screen Completions. Bachelor thesis at the University of Stavanger, Norway.
- Jones C, Morgan Q, Beare S, Awid A, Parry K (2009). Design, Testing, Qualification and Application of Orifice Based Inflow Control Devices. International Petroleum Technology Conference, Doha, Qatar, 7-9 December. IPTC-13292-MS.
- Lauritzen J, Shahreyar N, Jacob S (2011). Selection Methodology for Passive, Active, and Hybrid Inflow Control Completions. Offshore Technology Conference, Houston, Texas, USA, 2-5 May. OTC-21910-MS.
- Maclachlan S, Harper C (2016). A Holistic Approach to Sand Control. Presented at SPE Bergen One Day Seminar, Grieghallen, Bergen, Norway, 20 April. SPE-180046-MS.
- Marir B, Allouti A, Cobb D (2011). Simulation Modeling of ICDs and MLTBs in Green Field Offshore Abu Dhabi. SPE Reservoir Characterization and Simulation, Abu Dhabi, United Arab Emirates, 9-11 Oct. SPE-148075-MS.
- Minulina P, Al-Sharif S, Zeito G, Bouchard M (2012). The Design, Implementation and Use of Inflow Control Devices for Improving the Production Performance of Horizontal Wells. SPE International Production and Operations Conference and Exhibition, Doha, Qatar, 14-16 May. SPE-157453-MS.
- Neylon K, Reiso E, Holmes J, Nesse O (2009). Modeling Well Inflow Control with Flow in Both Annulus and Tubing. SPE Reservoir Simulation Symposium, The Woodlands, Texas, USA, 2-4 February. SPE-118909-MS.
- Ouyang L (2009). Practical Consideration of an Inflow-Control Device Application for Reducing Water Production. SPE Annual Technical Conference and Exhibition, New Orleans, Louisiana, 4-7 October. SPE-124154-MS.
- Raffn A, Zeybek M, Moen T, Lauritzen J, Sunbul A, Hembling D, Majdpoor A (2008). Case Histories of Improved Horizontal Well Cleanup and Sweep Efficiency with Nozzle-Based Inflow Control Devices in Sandstone and Carbonate Reservoirs. Offshore Technology Conference, Houston, Texas, USA, 5-8 May. OTC-19172-MS.
- Raffin A, Hundsnes S, Kvernstuen S, Moen T (2007). ICD Screen Technology Used To Optimize Waterflooding in Injector Well. Production and Operations Symposium, Oklahoma City, Oklahoma, U.S.A, 31 March to 3 April. SPE-106018-MS.
- Richardson J, Sangree J, Sneider R (1987). Coning. J. Petroleum Technology. 39: 08. SPE-15787-PA.
- Salamy S (2005). Maximum Reservoir Contact (MRC) Wells: A New Generation of Wells for Developing Tight Reservoir Facies. SPE Distinguished Lecturer Series. SPE-108806-DL.
- Shi H, Zhou H, Hu Y, He Y, Fu R, Ren B (2016). A New Method to Design and Optimize the ICD for Horizontal Wells. Offshore Technology Conference, Houston, Texas, USA, 2-5 May. OTC-26905-MS.
- Smith C, Dehghani A, Hatcher W, Mukhambetpaizov Y, Askarov B, Burg G (2016). Case Study: Kazakhstan's First Application of Inflow Control Devices ICDs for Horizontal Wells. IADC/SPE Asia Pacific Drilling Technology Conference, Singapore 22-24 August. SPE-180639-MS.
- Thornton K, Soliman M, Jorquera R (2010). Optimization of Inflow Control Device Placement and Mechanical Conformance Decisions Using a New Coupled Well-Intervention Simulator. SPE Latin American and Caribbean Petroleum Engineering Conference, Lima, Peru, 1-3 December. SPE-139435-MS.
- Vasper A, Gurses S (2013). Optimized Modeling Workflows for Designing Passive Flow Control Devices in Horizontal Wells. SPE Reservoir Characterization and Simulation Conference and Exhibition, Abu Dhabi, UAE 16-18 September. SPE-166052-MS.
- Wang J, Dale B, Ellison T, Benish T, Grubert M (2008). Coupled Well and Reservoir Simulation Models to Optimize Completion Design and Operations for Subsurface Control. Europec/EAGE Conference and Exhibition, Rome, Italy, 9-12 June. SPE-113635-MS.
- Youl K, Harkomoyo H, Suhana W, Regulacion R, Jorgensen T (2011). Passive Inflow Control Devices and Swellable Packers Prove to Control Water Production in Fractured Carbonate Reservoir: A Comparison with Slotted Liner Completions. SPE/IADC Drilling Conference and Exhibition, Amsterdam, Netherlands, 1-3 March. SPE-140010-MS.

Full Length Research Paper

Analysis and field applications of water saturation models in shaly reservoirs

Shedid A. Shedid* and Mohamed A. Saad

American University in Cairo (AUC), New Cairo, The 90th Avenue, P. O. 11837, Cairo, Egypt.

Received 25 May, 2017; Accepted 5 September, 2017

Shaly sandstone reservoirs have complex pore systems with ultra-low to low interparticle permeability and low to moderate porosity. This has led to development of several models to calculate water saturation in shaly sandstone reservoirs using different approaches, assumptions and certain range of conditions for application. This study has used actual well logging data from two different fields of South Texas and North Sea to evaluate and compare the most popular five shaly sandstone models for calculating water saturation. Furthermore, sensitivity analysis of tortuosity coefficient (α), cementation exponent (m) and water saturation exponent (n) is achieved to investigate their effects on computed values of water saturations using different models. The results indicated that the increase of shale volume decreases water saturation calculated for all popular models. In addition, the increase of tortuosity coefficient and/or cementation exponent (m) causes overestimation of water saturation while the increase of saturation exponent (n) results in underestimation values. The results also showed that the increase of shale volume decreases water saturation calculated for all popular models. In addition, the increase of tortuosity coefficient and/or cementation exponent (m) causes overestimation of water saturation while the increase of saturation exponent (n) results in underestimation values.

Key words: Shaly reservoirs, water saturation, well logging, field analysis.

INTRODUCTION

Development of shaly reservoirs represents a real challenge in the oil industry due to their severe heterogeneity and complex nature. The calculation of irreducible water saturation (S_{wi}) is essential to calculate the oil saturation ($S_o = 1 - S_{wi}$), which is imperative in calculating hydrocarbon volumes.

The existence of clay minerals in oil and gas reservoirs complicates the calculation of water saturation using Archie's equation (Archie, 1942). This is because the

behavior of the clay particles depends mainly on shale type and its distribution in the pore space which contributes to the electrical conductivity of the formation.

Many models have been developed to calculate the water saturation in shaly sandstone formation considering the shale type and its distribution. Applying different approach of each water saturation model has led to different values of water saturation being calculated. This may cause drastic erroneous values of calculated

*Corresponding author. E-mail: shedid2020@yahoo.com

hydrocarbon volumes.

WATER SATURATION MODELS IN CLEAN-AND SHALY RESERVOIRS

Clean-sand reservoirs

Archie (1942) proposed the most popular and widely used model to determine water saturation in clean sand zones. This model was mainly developed using a theoretical approach for clean sandstone and carbonates having zero shale volume. Therefore, application of Archie's model requires special consideration for the resistivity data used. Archie's model was given by the following equation:

$$S_w = \left(\frac{a R_w}{\phi^m R_t} \right)^n \quad (1)$$

Where a is the tortuosity factor, m is the Archie cementation constant, n is the Archie saturation exponent, R_w is the brine water resistivity at formation temperature (Ωm), R_t is true resistivity of uninvaded deep formation (Ωm), and ϕ is the total porosity (%).

Shale is defined as a clay-rich heterogeneous rock that contains variable content of clay minerals (mostly illite, kaolinite, chlorite, and montmorillonite) and organic matter (Brock, 1986; Mehana and El-Monier, 2016). The absence of shale characteristics in the above-Archie's equation (Equation 1) reveals that Archie's equation was not designed and cannot be used for shaly sand formations. The presence of clay in the formation complicates the interpretation and may give misleading results if Archie's equation is used because the clay is considered to be a conductive medium. Therefore, several models were developed for calculating water saturation in shaly formations. These models were evaluated and compared in this study, as presented below.

Shaly sand reservoirs

Presence of shale in the formation has been considered as a very disturbing factor and shows severe effects on petrophysical properties due to reduction in effective porosity, total porosity and permeability of the reservoir (Ruhovets and Fertl, 1982; Kamel and Mohamed, 2006). Moreover, the existence of shale causes uncertainties in formation evaluation, proper estimation of oil and gas reserves, and reservoir characterization (Shedid et al., 1998; Shedid, 2001; Shedid-Elgaghah et al., 2001).

For shaly sandstone reservoirs, different models have been developed depending on different factors, such as; (1) input parameters and their sources, viz; routine core analysis, special core analysis and well logging data; (2)

development approach such as field or laboratory based, empirical or theoretical correlation, and (3) shale distribution and the model's dependency on types as laminar, structural or dispersed. Different shale distributions inhibit different electric conductivity, permeability, and porosity. The distribution of clay within porous reservoir formations can be classified into three groups (Glover, 2014), as illustrated in Figure 1:

- (1) Laminated: Thin layers of clay between sand units.
- (2) Structural: Clay particles constitute part of the rock matrix, and are distributed within it.
- (3) Dispersed: Clay in the open spaces between the grains of the clastic matrix.

In this study, the five popular shaly sand water saturation models are evaluated and compared using actual field well logging data. Furthermore, sensitivity analysis of the effects of coefficients (a , m , and n) involved in these models on computed water saturation is undertaken.

Laminated shale model

Poupon et al. (1954) developed a simplified model to determine water saturation in laminated shaly sand formations. Their approach described shale as multiple thin parallel layers of 100% shale interbedded with clean-sand layers within the vertical resolution of the resistivity-logging tool. The laminated shale does not affect the porosity or permeability of the sand streaks themselves. However, when the amount of laminar shale is increased and the amount of porous medium is correspondingly decreased and finally overall porosity is reduced in proportion, this model is given by the following equation:

$$S_w = \sqrt{\frac{a R_w (1 - V_{sh})}{\phi^m} \left(\frac{R_{sh} - V_{Lam} R_t}{R_t R_{sh}} \right)} \quad (2)$$

Where R_{sh} is the average value of the deepest resistivity curve reading in shale (Ωm), V_{sh} is volume of shale in the formation (%), V_{Lam} is the volume of laminated shale in the formation (%), and ϕ is the total porosity (%).

Dispersed shale model

Dispersed shale distribution is composed of clay minerals that form in-place after deposition due to chemical reactions between the rock minerals and the chemicals in the formation water. The dispersed shale is composed of clay particles, fragments or crystals to be found on grain surface that occupy void spaces between matrix particles and reduce the effective porosity (ϕ_e) and permeability significantly.

De Witte (1950) developed a model for estimating water saturation in dispersed shaly sand formations. He assumed that the formation conducts electrical current

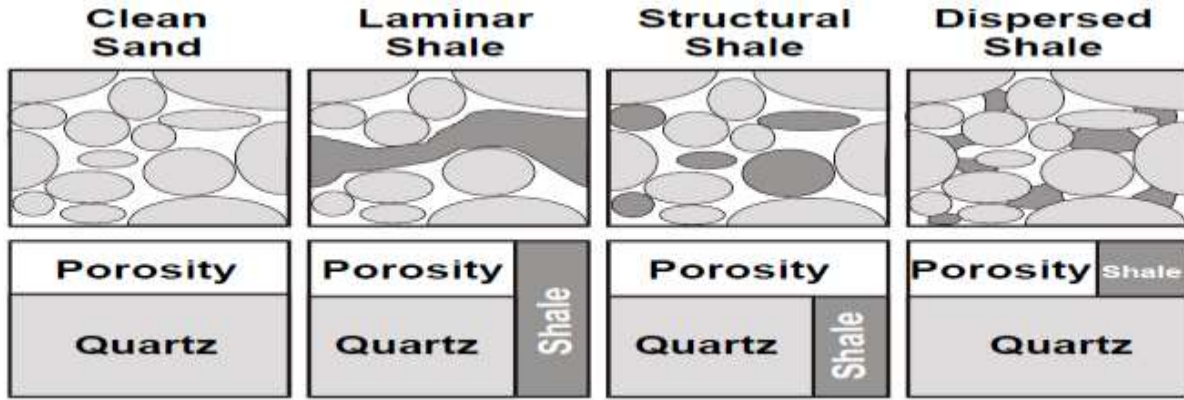


Figure 1. Different shale distribution modes.
Source: Glover (2014).

through a network composed of the pore water and dispersed clay. The dispersed shale in the pores markedly reduces the permeability of the formation. This model is given by the following equation:

$$S_w = \frac{1}{1-q} \sqrt{\frac{a R_w}{\phi_{im}^2 R_t} + \frac{q^2}{4} - \frac{q}{2}} \quad (3)$$

Where ϕ_{in} is the inter-matrix porosity (%), which is assumed to be equal to sonic porosity in shaly sand (%). The parameter q is called the sonic response and for dispersed shale distribution response, q could be described as:

$$q = \frac{\phi_s - \phi_D}{\phi_s} \quad (3a)$$

Where ϕ_s is sonic porosity (%) and ϕ_D is density porosity (%).

Simandoux's model

Simandoux (1963) developed a model for estimating water saturation in shaly sand formation. The model was a result based on laboratory studies performed on a physical reservoir model composed of artificial sand and clay in the laboratories of the Institute of French Petroleum (IFP). Simandoux model remains one of the most popular, shaly sand water saturation models, and a highly influential framework for later studies in this field. The Simandoux equation works regardless of shale distribution and is given by the following equation:

$$S_w = \frac{a R_w}{2 \phi^m} \left[\left(\frac{-V_{sh}}{R_{sh}} \right) + \sqrt{\left(\frac{V_{sh}}{R_{sh}} \right)^2 + \left(\frac{4 \phi^m}{a R_w R_t} \right)} \right] \quad (4)$$

All parameters involved in the above equation are defined above for the previously-listed models/equations.

Indonesian equation

Poupan and Leveaux (1971) developed a model to determine water saturation in laminated shaly formations. This model is widely known as the Indonesian equation. The Indonesia model was developed by field observation in Indonesia, rather than by laboratory experimental measurement support. The Indonesian equation remains a benchmark for field-based models that work reliably with log-based analysis regardless of special core analysis data. It also does not particularly assume any specific shale distribution. The Indonesian model also has an extra feature as the only model that considers the saturation exponent (n). This model is given by the following equation:

$$\frac{1}{R_t} = S_w^{n/2} \left(\frac{V_{sh}^{1-V_{sh}/2}}{\sqrt{R_{sh}}} + \left(\frac{\phi^{m/2}}{\sqrt{a R_w}} \right) \right) \quad (5)$$

In addition, according to Poupan and Leveaux (1971), satisfactory results have been obtained in some cases with a somewhat simpler equation, which is more convenient for quick interpretation. This equation simply eliminates the $(1-V_{sh}/2)$ exponent, yielding the following equation:

$$S_w = \frac{1}{R_t} \left(\frac{\sqrt{a R_w R_{sh}}}{V_{sh} \sqrt{a R_w} + \phi^{m/2} \sqrt{R_{sh}}} \right)^{n/2} \quad (6)$$

All parameters of the above equation are defined above for the previous equations.

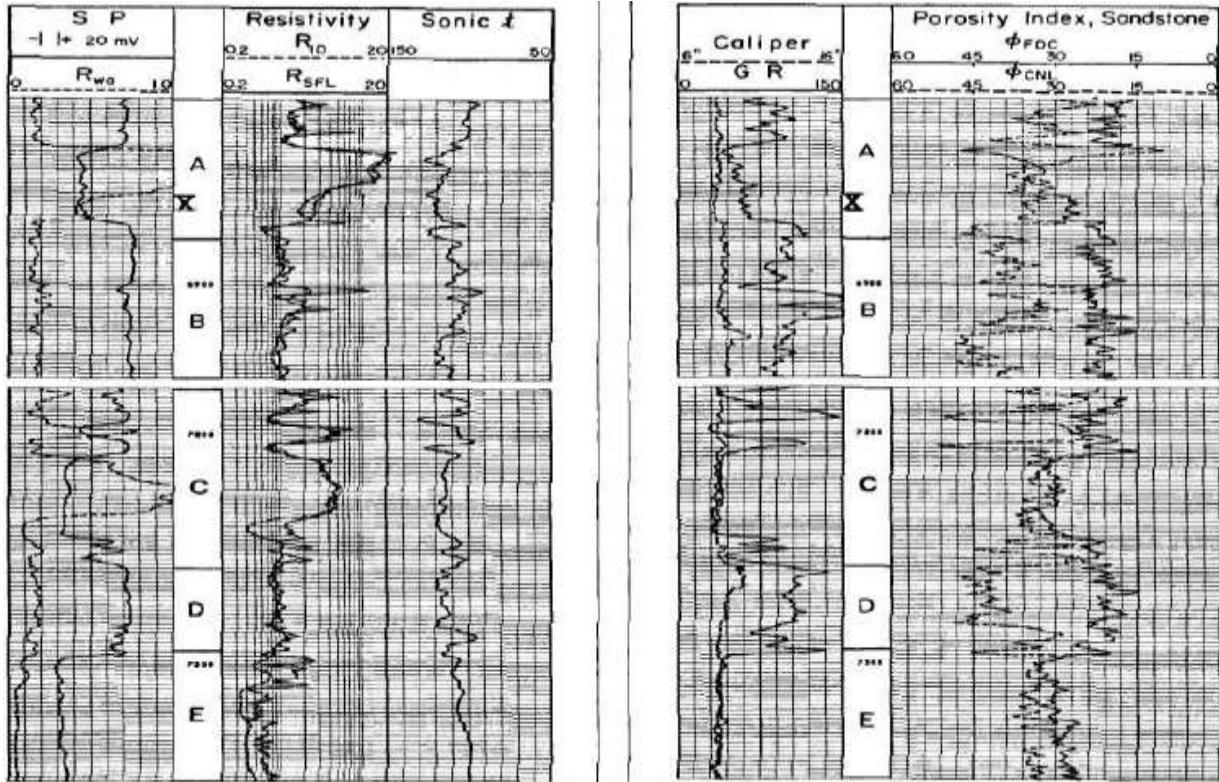


Figure 2. Well log from South Texas field. Source: Best et al. (1978).

Total shale model

Schlumberger developed a model for estimating water saturation in shaly sand formation, which is called the total shale model (Schlumberger, 1972). Based upon the previous laboratory investigations proposed by Simandoux (1963), and field experience conducted on the Niger Delta as presented by Poupon et al. (1967), Schlumberger (1972) model is suitable for many shaly formations, independent of the distribution of the shale or the range of water saturation values encountered in the log analysis. However, it is notable that although the total shale model originates from the Simandoux equation, it does not consider the cementation factor (m), which reduces its accuracy relatively to the Simandoux equation. The total shale model is considered a highly practical and simple model that has been frequently modified for further studies and processes. This model is given by the following equation:

$$S_w = \frac{aR_w(1-V_{sh})}{2\phi^2} \left[\left(\frac{-V_{sh}}{R_{sh}} \right) + \sqrt{\left(\frac{V_{sh}}{R_{sh}} \right)^2 + \left(\frac{4\phi^2}{aR_wR_i(1-V_{sh})} \right)} \right] \quad (7)$$

All parameters included in Equation 7 are defined above for the previous equations.

FIELD APPLICATIONS FOR COMPARING WATER SATURATION MODELS IN SHALY RESERVOIRS

Actual well logs from South Texas and North Sea fields are used to investigate and compare the five water saturation models in shaly sand reservoirs. The well logging-derived data are used to calculate water saturation, identify shale distribution and perform sensitivity analysis for different models.

South Texas field

The average reservoir temperature for the South Texas field was reported to be 150°F, and the Neutron log reported sandstone lithology while the SP and GR logs indicated different proportions of shales. The South Texas section of interest has been divided into four intervals. Interval A contains shaly hydrocarbon-bearing sand, which has a gas cap indicated by separation of the neutron and density porosities. Interval B is mostly shale with some thin sands and can be used to select shale parameters. Interval C contains hydrocarbon-bearing sands while Interval D contains reasonably clean water sand, as presented by Best et al. (1978) in Figure 2.

To help in identification of shale distribution mode and to use it for selection of the suitable model for calculating

Table 1. Constants and measured parameters for the South Texas Well.

Depth (ft)	SP (mv)	GR (API)	Rt (Ω m)	ϕ N	ϕ D	Δt (μ s/ft)	ϕ S	q	Vsh SP	Vsh GR	ϕ
6880	15.50	105.00	0.90	0.36	0.19	113.00	0.41	0.53	0.95	0.61	0.28
6886	15.00	95.00	1.00	0.44	0.27	112.00	0.40	0.33	0.90	0.52	0.36
6892	15.50	83.00	1.20	0.36	0.21	105.00	0.36	0.41	0.95	0.42	0.29
6898	15.00	87.00	1.00	0.42	0.17	110.00	0.39	0.57	0.90	0.45	0.30
6904	14.50	135.00	2.00	0.42	0.23	110.00	0.38	0.39	0.85	0.87	0.33
6910	14.00	105.00	1.80	0.28	0.21	104.00	0.34	0.38	0.80	0.61	0.25
6916	15.00	120.00	1.00	0.39	0.21	110.00	0.38	0.45	0.90	0.74	0.30
6922	14.00	100.00	0.95	0.46	0.23	119.00	0.45	0.49	0.80	0.57	0.35
6928	14.50	88.00	0.80	0.43	0.19	120.00	0.47	0.59	0.85	0.46	0.31
6934	14.50	95.00	0.90	0.36	0.23	117.00	0.44	0.48	0.85	0.52	0.30
6940	15.00	98.00	1.00	0.39	0.21	110.00	0.39	0.46	0.90	0.55	0.30

Constants and parameters used: $a^* = 1.55$, $n^* = 2.00$, $m^* = 1.68$, $GR_{max} = 150.0$ API, $GR_{min} = 35.0$ API, $R_{wa} = 0.04$ Ω m, $R_{wsh} = 1.80$ Ω m, $R_w = 0.04$ Ω m, $R_{wsh} = 0.40$ Ω m, $\Delta t_{matrix} = 55.50$ μ ft/s, $\Delta t_f = 189$ μ ft/s, $\Delta t_{sh} = 60.0$ μ ft/s, $\Delta \rho_{matrix} = 2.65$ g/cm³, $\Delta \rho_{shale} = 2.60$ g/cm³, $\Delta \rho_{fluid} = 1.0$ g/cm³. Where R is resistivity (Ω m), Δt = measured log sonic travel time (μ s/ft), $\Delta \rho_{matrix}$, $\Delta \rho_{matrix}$ matrix = fluid and shale density, respectively (g/cm³).

Table 2. Calculated water saturation using five different shaly sand models for the South Texas field.

Depth (ft)	S_w Laminated	S_w Dispersed	S_w Indonesian	S_w Total shale	S_w Simandoux
6880	0.405	0.901	0.606	0.537	0.680
6886	0.346	0.692	0.476	0.445	0.537
6892	0.423	0.773	0.481	0.551	0.587
6898	0.445	0.929	0.555	0.569	0.627
6904	0.030	0.499	0.223	0.175	0.359
6910	0.236	0.612	0.325	0.405	0.497
6916	0.268	0.828	0.491	0.383	0.587
6922	0.345	0.708	0.503	0.447	0.561
6928	0.487	0.887	0.668	0.607	0.679
6934	0.435	0.753	0.599	0.559	0.655
6940	0.384	0.817	0.528	0.506	0.608

water saturations in the South Texas field, readings are obtained from sections of interest of the logs from a well in the South Texas field (Best et al., 1978), as shown in Figure 2. Shaly sand sections are corresponding to depths 6,880 ft to 6,940 ft in the well. For this shaly sand section, the corresponding parameters are read at 10 different depths and used to calculate water saturation using different shaly sand models.

The parameters and well logging readings are used in the comparison of water saturation models and listed below in Table 1. The Gamma ray values are used in shale volume (V_{sh}) calculations because it indicates lower values for shale volume than those from the SP log, Table 1. The total porosity (ϕ) is calculated as a mathematical average of neutron and density porosities (ϕ_N and ϕ_D), respectively.

The modified resistivity factor (F^*) for shaly formation is plotted versus porosity. This is known as a modified Picket plot of $\log(F^*)$ versus $\log(\phi)$. This plot is used to

obtain values for modified tortuosity (a^*) and modified exponent (m^*) for shaly formation of this field. The value of a^* is obtained as the value of ϕ at the intersection of the x-y axis, and m^* is obtained as negative slope of the line in the log-log plot.

The parameter q involved in the dispersed shale model is called the sonic response and is calculated using values of sonic and density porosity as; $\{q = (\phi_s + \phi_D) / \phi_s\}$. The data listed in Table 1 is used to compute water saturation using five shaly sand water saturation models and the results attained are presented in Table 2. The calculated values of shale volume and water saturation are graphically presented in Figure 3. Figure 3 compares the shale volume and water saturation (S_w) values using five different models as a function of depth in the shaly sand zones of the South Texas field.

For the South Texas field, as shown in Figure 3, the dispersed shale model overestimates values of water saturation, while the laminated shale model provides

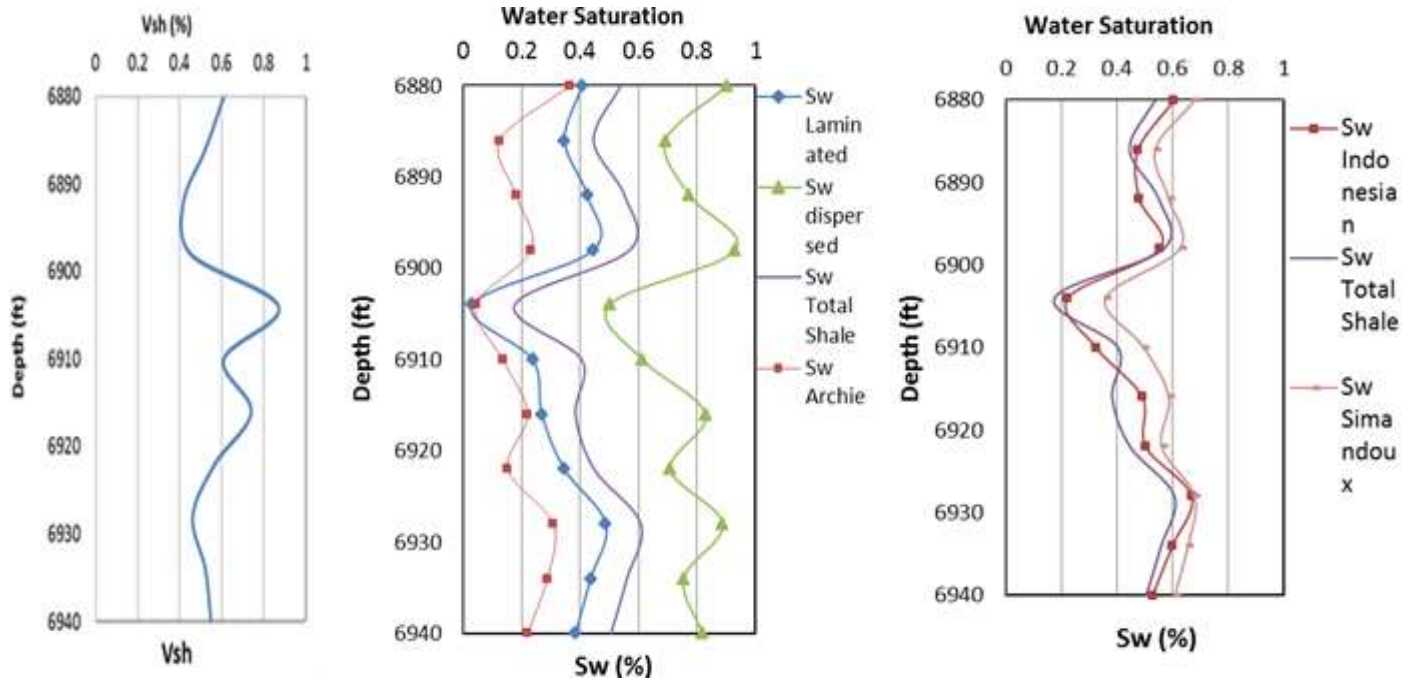


Figure 3. Comparison of shale volume and shaly sand water saturation models for South Texas field.

underestimated values, relatively to the total shale model, which is indifferent to shale distribution.

Although there is a big difference in the values of the dispersed shale model and the laminated shale model, however, they followed a similar responsiveness and pattern to the total shale model and shale volume (V_{sh}) curve. This may reveal that both laminated and dispersed distributions exist homogeneously in the South Texas field. This conclusion is based on the fact that the average of the laminated and dispersed shale models resulted averagely to the curves of the remaining shaly sand water saturation models, which takes all shale distribution modes into account.

The results of the total shale model, Simandoux equation, and Indonesian model show very similar values overall with insignificant variance in the results (Figure 3). This similarity between these three models may indicate proper estimation of the values of tortuosity factor (α), cementation factor (m), and saturation exponent (n). It also indicates the applicability of all three models for the South Texas field.

Based on the results attained from comparing different water saturation models, it is imperative to identify the shale distribution in the formation to select the appropriate model for accurate calculations. For identification of shale distribution, the technique of plotting the porosity derived from neutron and density logs is applied (Institute of Petroleum Engineering (IPE), 2014). The actual data from the South Texas well is plotted on this triangle and location of plotted data indicates the distribution mode of shale. This crossplot of

neutron (ϕ_N) - density (ϕ_D) porosity is presented in Figure 4.

Figure 4 has been used in the oil industry to identify the shale distribution mode. It is mainly a plot of density porosity versus neutron porosity on y and x axes, respectively. Distribution of data points in Figure 4 indicates that the South Texas field exhibit both laminated and structural shale distribution homogeneously across the reservoir. This means using another saturation model rather than laminated one provides erroneous results.

North Sea field

Actual well log from the North Sea field is presented by Institute of Petroleum Engineering (IPE) (2014), as shown in Figure 5. The shaly sand sections of interest correspond to depths from 11,870 to 11,880 ft in the North Sea field. For shaly sand sections, the corresponding parameters are read at 10 different depths, and used to calculate water saturation using five different shaly sand models.

Readings of different well logs plus constants and parameters for the shaly sand zones are listed versus depth in Table 3. Five different shaly sand models are used to calculate the water saturation and the obtained results are listed in Table 4 for the North Sea field and graphically presented in Figure 6. Figure 6 compares the attained values of water saturation computed using different models versus depth in the shaly sand zones

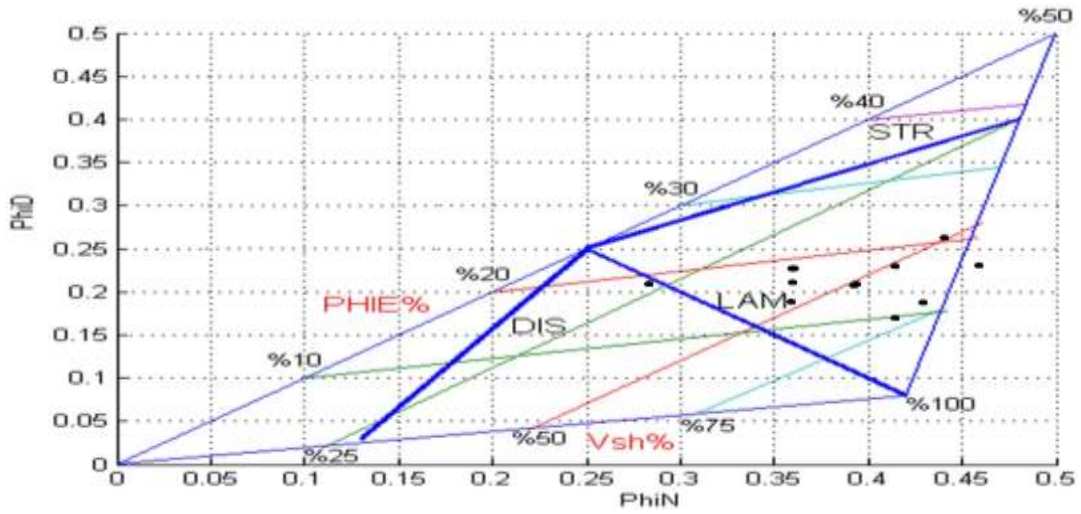


Figure 4. Crossplot of neutron porosity (ϕ_N) vs. density porosity (ϕ_D) for the South Texas well showing shale distribution.

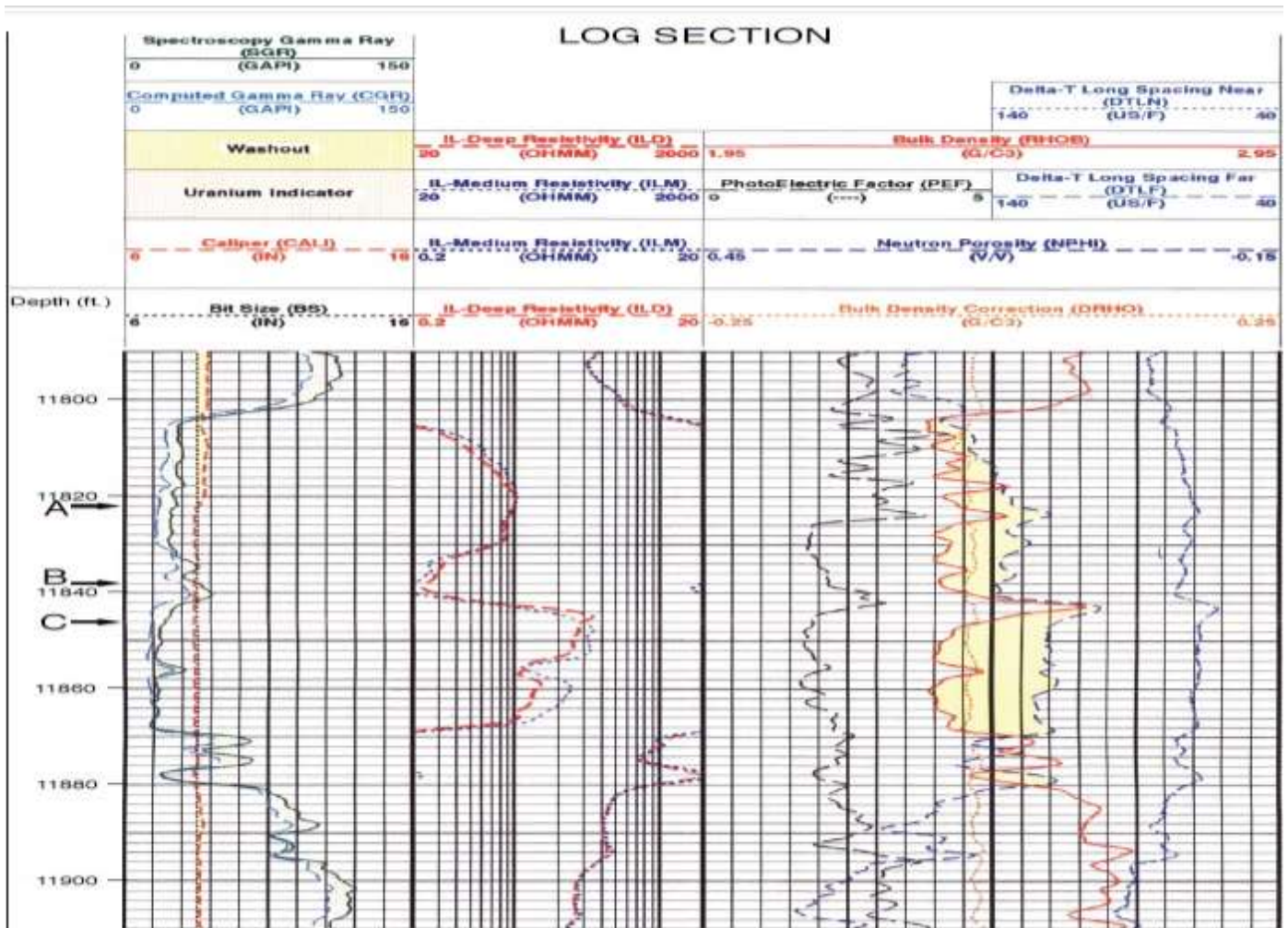


Figure 5. Well log from North Sea. Source: Wylie et al. (1955).

Table 3. Constants and measured parameters for the North Sea well.

Depth (ft)	ρ (g/cm ³)	GR (API)	Rt (Ω m)	ϕ N	ϕ D	Δt (μ s/ft)	ϕ S	q	Vsh GR	ϕ
11870	2.49	66.00	13.00	0.14	0.08	113.00	0.41	0.80	0.54	0.11
11871	2.51	73.00	10.00	0.17	0.07	112.00	0.40	0.83	0.61	0.12
11872	2.49	63.00	9.00	0.15	0.08	105.00	0.35	0.77	0.51	0.12
11873	2.45	63.00	8.00	0.12	0.11	110.00	0.39	0.73	0.51	0.11
11874	2.49	67.00	7.00	0.15	0.08	110.00	0.39	0.79	0.55	0.12
11875	2.56	72.00	7.00	0.17	0.04	104.00	0.34	0.89	0.60	0.10
11876	2.54	45.00	10.00	0.18	0.06	110.00	0.40	0.86	0.32	0.12
11877	2.43	48.00	16.00	0.15	0.12	119.00	0.46	0.73	0.35	0.14
11878	2.39	45.00	20.00	0.10	0.15	120.00	0.47	0.69	0.32	0.12
11879	2.43	40.00	14.00	0.09	0.13	117.00	0.45	0.72	0.26	0.11
11880	2.48	37.00	8.00	0.10	0.10	110.00	0.40	0.76	0.23	0.10

Constants and parameters used: $a^* = 1.65$, $n^* = 2.00$, $m^* = 1.33$, $GR_{max} = 110.0$ API, $GR_{min} = 15.0$ API, $R_{wa} = 0.04$ Ω m, $R_{sh} = 18.0$ Ω m, $R_w = 1.8$ Ω m, $R_{wsh} = 0.40$ Ω m, $\Delta t_{matrix} = 55.50$ μ f/s, $\Delta t_{fluid} = 189$ μ f/s, $\Delta t_{sh} = 60.0$ μ f/s, $\Delta\rho_{matrix} = 2.65$ g/cm³, $\Delta\rho_{shale} = 2.60$ g/cm³, $\Delta\rho_{fluid} = 1.0$ g/cm³.

Table 4. Calculated water saturation using five different shaly sandstone models for the North Sea field.

Depth (ft)	S_w Laminated	S_w Dispersed	S_w Indonesian	S_w Total shale	S_w Simandoux
11870	0.1642	0.1821	0.0750	0.4033	0.2905
11871	0.1705	0.2812	0.0922	0.3987	0.3174
11872	0.2183	0.3037	0.1060	0.4867	0.3430
11873	0.2398	0.2509	0.1211	0.5305	0.3707
11874	0.2438	0.3489	0.1355	0.5336	0.3911
11875	0.2434	0.7751	0.1426	0.5548	0.4175
11876	0.2519	0.3225	0.0983	0.5392	0.3256
11877	0.1622	0.0954	0.0560	0.3586	0.2327
11878	0.1534	0.0669	0.0478	0.3582	0.2210
11879	0.2349	0.1107	0.0766	0.5290	0.2974
11880	0.3533	0.2612	0.1412	0.7789	0.4163

of interest of the North Sea field.

For the North Sea field, as shown in Figure 6, the Indonesian shale model yielded the lowest values of water saturation (S_w) while the total shale model provided exceptionally the highest values. This figure also presented the water saturation calculated using Archie's equation, which lies in the middle between these two extreme cases. As for the same graph (Figure 6), the total shale model also gave high estimates of S_w , while the Simandoux equation showed slighter lower values, and the Indonesian model shows very low values of S_w . This highly estimated value using the total shale model is mostly attributed to the generous assumption in the total shale model that $m = n = 2$ for all reservoirs. This shows that proper estimation of the values of m and n have a real impact on the estimated water saturation values. This big variance between the total shale model, Simandoux equation, and Indonesian model, may indicate poor attribution for the estimated values of tortuosity factor (a), cementation factor (m), and

saturation exponent (n). This may be caused due to the poor estimate of water resistivity (R_w).

The calculated water saturation (S_w) using the dispersed shale model between depths 11,873 and 11,876 ft in Figure 6 shows an extreme boost in values of S_w that occurred with the sudden increase in shale volume (V_{sh}) which could be described as an abnormality. This may be attributed to improper selection of the dispersed shale model for this particular field. On the other hand, the laminated shale model followed an almost similar responsiveness and pattern to the remaining water saturation models in shaly sand, particularly the total shale model.

It is essential to properly describe shale distribution and verify the quality and accuracy of input parameters in order to select the correct shaly sand model for calculation of water saturation. The neutron-density porosity crossplot of the North Sea field is presented in Figure 7 and used to identify the shale distribution in the North Sea field.

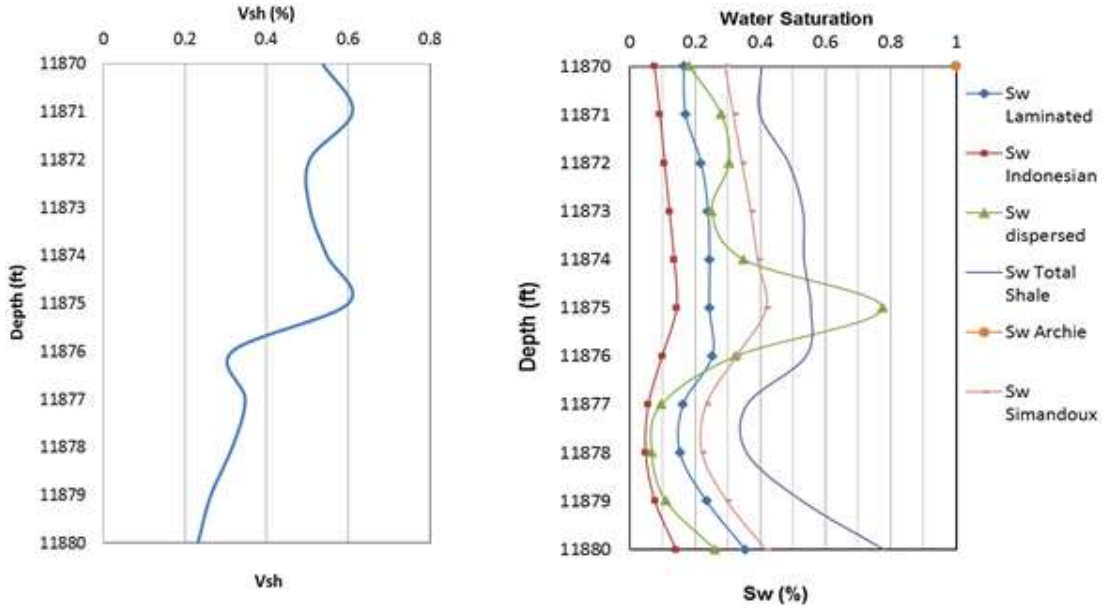


Figure 6. Comparison of shaly sand water saturation models for the North Sea field.

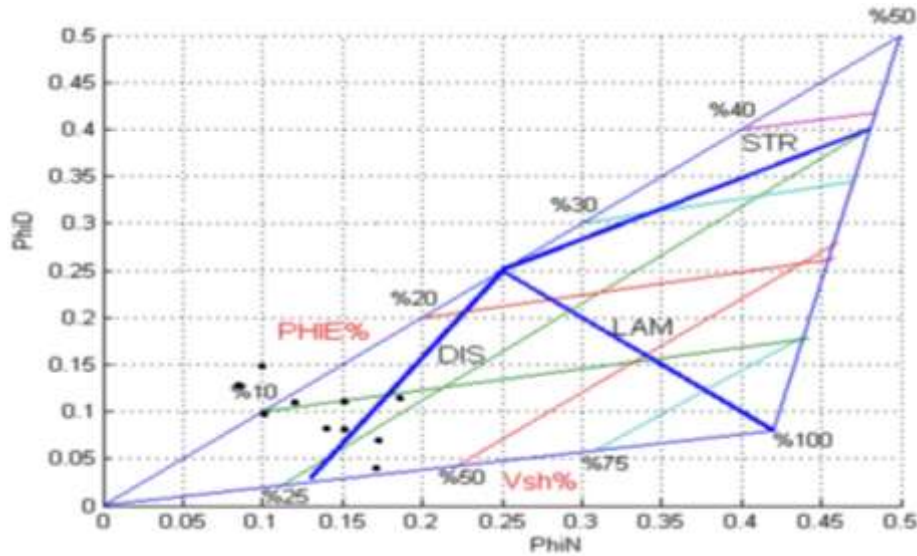


Figure 7. Crossplot of neutron porosity (ϕ_N) versus density porosity (ϕ_D) for the North Sea well showing shale distribution.

The plot of Figure 7 indicates that North Sea field mostly inhibits dispersed shale distribution.

SENSITIVITY ANALYSIS OF a, m AND n EXPONENTS OF WATER SATURATION MODELS

Variation of the tortuosity coefficient (a), cementation exponent (m) and saturation exponent (n) has been

studied. A sensitivity analysis is carried out to study the effect of applying different values of a and m on values of water saturation using the laminated shale model. The Indonesian model is used to study the effect of saturation exponent (n) because it is the only model involving that exponent (n).

Figure 8 graphically presents the calculated values of water saturation using different values of tortuosity coefficient (a) versus depth for all-selected models. A

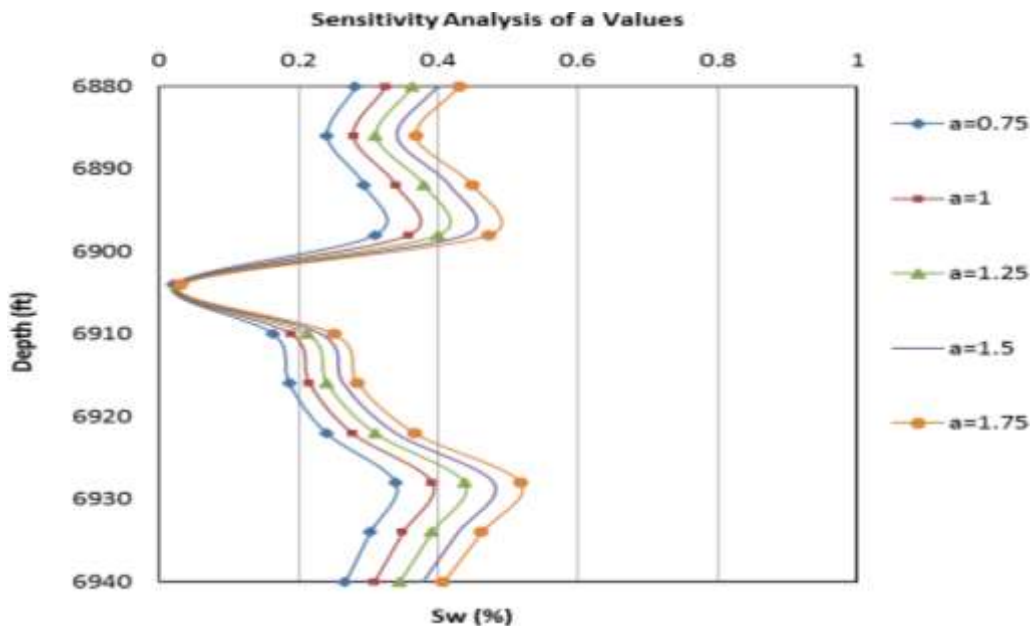


Figure 8. Effect of tortuosity coefficient (a) on computed water saturations for the South Texas field (laminated shale model).

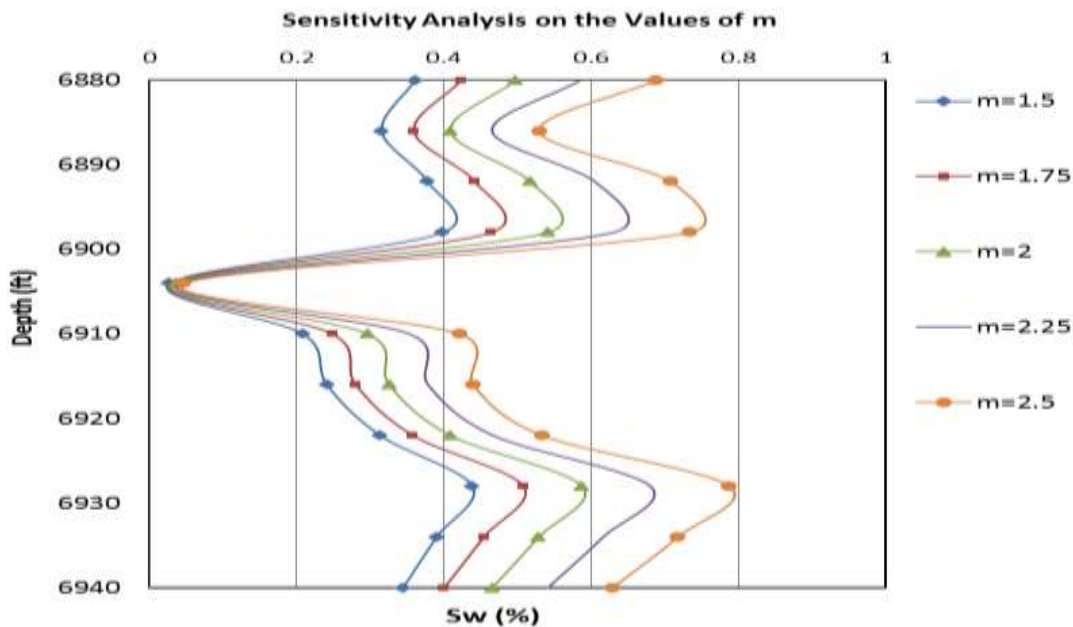


Figure 9. Effect of cementation exponent (m) on computed water saturations for the South Texas field (laminated shale model).

conclusion can be drawn that the increase of tortuosity coefficient (a) results in an increase in calculated values of water saturation for all shaly sand models.

The effect of variable values of the cementation exponent (m) on water saturation versus depth is achieved and the results are plotted in Figure 9 which

reveals that the increase of m values increases the computed values of water saturation in shaly sandstone reservoirs.

The Indonesian water saturation model is used to perform a sensitivity analysis about the effect of applying different values of the saturation exponent (n) on the

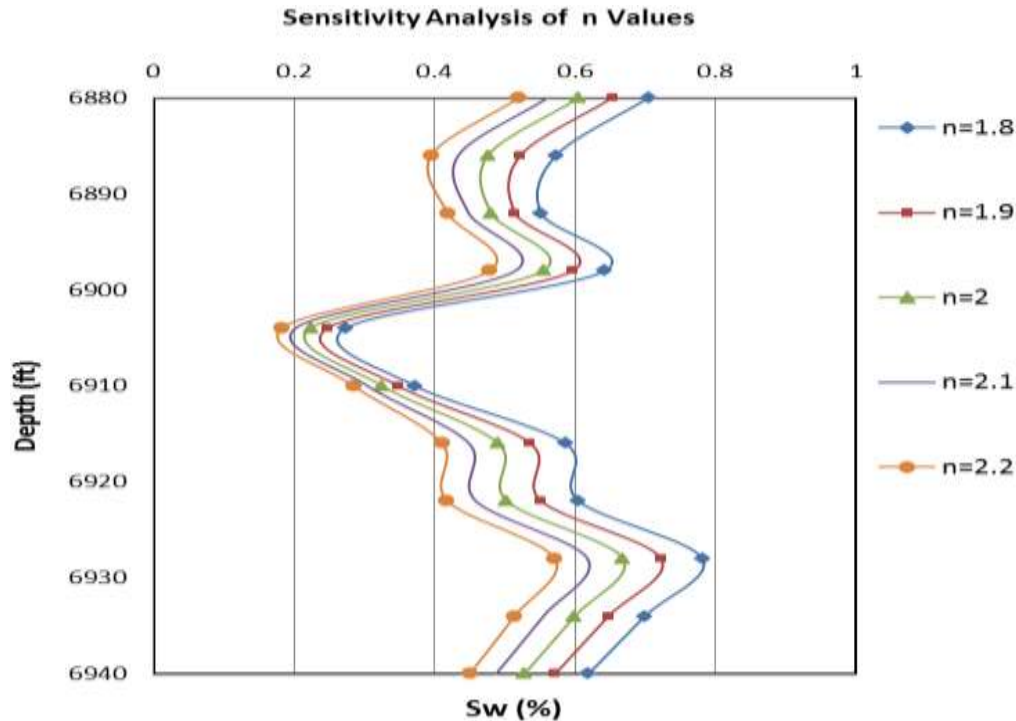


Figure 10. Effect of saturation exponent (n) on computed water saturations for the South Texas field (Indonesian model).

saturation values calculated. The results are presented in Figure 10. The increase of cementation exponent (m) causes an increase in water saturation calculated using the Indonesian model.

The increase of saturation exponent (n) leads to an increase in water saturation calculated (Figure 10). A simple comparison of the effects of n , m , and n on water saturation (Figures 8, 9 and 10), respectively, indicates that the m exponent has the highest impact while the tortuosity factor (a) has the lowest one.

Conclusion

Comparison and evaluation of different shaly sand models is achieved and sensitivity analysis of the tortuosity factor, cementation and saturation exponents is carried out in this study. The attained conclusions are summarized as follows:

- (1) Identification of the shale distribution in the reservoir is crucial for selecting the appropriate model for calculating the water saturation in shaly sand reservoirs.
- (2) The increase of shale volume decreases the calculated values of water saturation using all shaly sand models.
- (3) Different shaly sand water saturation models inhibit a drastic variance in estimated water saturation which may exceed 60% in difference.

(4) The laminated shale model provides the lowest value of water saturation while the total shale model produces the highest one.

(5) Application of Simandoux, Indonesian and total shale models provides comparable results of water saturation in shaly sand reservoirs.

(6) Overestimation of the tortuosity factor (a) and cementation exponent (m) causes an overestimation of water saturation calculated using all models.

(7) Overestimation of the saturation exponent (n) results in an underestimation of water saturation calculated using all models.

(8) Total shale model showed the highest degree of responsiveness to variance in shale volume of all shaly sand water saturation models.

NOMENCLATURE

a , tortuosity factor, unitless; GR , Gamma Ray log value, API; M , cementation constant, unitless; n , water saturation exponent, unitless; a^* , tortuosity factor for shaly rocks, unitless; m^* , cementation constant for shaly reservoirs, unitless; n^* , water saturation exponent for shaly reservoirs, unitless; R_w , brine water resistivity at formation temperature (Ωm); R_t , true resistivity of uninvaded deep formation (Ωm); R_{sh} , average value of the deepest resistivity curve reading in shale (Ωm); R_{sh} , average value of the deepest resistivity curve reading in

shale (Ω_m); \mathbf{q} , sonic response in dispersed shale model, dimensionless; **SP**, Spontaneous potential log; Δt , measured log sonic travel time ($\mu\text{s}/\text{ft}$); \mathbf{V}_{lam} , volume of laminated shale in the formation (%); \mathbf{V}_{sh} , shale volume in the formation (%).

Symbols

ϕ , Total porosity (%); ϕ_D , density porosity (%); ϕ_{im} , inter-matrix porosity (%); ϕ_s , sonic porosity (%); ρ , density (g/cm^3); $\Delta\rho_{\text{matrix}}$, matrix density (g/cm^3); $\Delta\rho_{\text{fluid}}$, fluid density (g/cm^3); $\Delta\rho_{\text{shale}}$, shale density (g/cm^3); Δt , measured log sonic travel time ($\mu\text{s}/\text{ft}$).

Subscript/Superscript


Sh, shale; **W**, water; **Lam**, laminated.

CONFLICT OF INTERESTS

The authors have not declared any conflict of interests.

REFERENCES

- Archie GE (1942). The Electrical Resistivity Log as an Aid in Determining Some Reservoir Characteristics. SPE J. 146:54-62.
- Best DL, Gardner JS, Dumanoir JL (1978). A Computer-Processed Wellsite Log Computation. Presented at the SPWLA 19th Annual Logging Symposium, El Paso, Texas, 13 -16 June. SPWLA- Z.
- Brock J (1986). Applied open-hole log analysis. Gulf Publishing Company, Texas, USA.
- DeWitte L (1950). Relations between resistivities and fluid contents of porous rocks. Oil Gas J. 49(16):120-134.
- Glover P (2014). The effect of clay on porosity and resistivity logs. In Petrophysics MSc Course Notes Chapt. 20. Yorkshire, United Kingdom: Leeds University.
- Institute of Petroleum Engineering (IPE) (2014). A Reservoir Sequence in the UKCS of the North Sea, Course Manual, London, United Kingdom.
- Kamel MH, Mohamed MM (2006). Effective porosity determination in clean/shaly formations from acoustic logs. J. Pet. Sci. Eng. 51(3-4):267-274.
- Mehana M, El-Monier L (2016). Shale characteristics impact on Nuclear Magnetic Resonance (NMR) fluid typing methods and correlations. Petroleum 2(2):138-147.
- Poupon A, Leveaux J (1971). Evaluation of Water Saturation in Shaly Formations, the SPWLA 12th Annual Logging Symposium, Dallas, Texas, 2-5 May. SPWLA-1971-O.
- Poupon A, Loy ME, Tixier MP (1954). A Contribution to Electrical Log Interpretation in Shaly Sands. J. Pet. Technol. 6(6):27-34.
- Poupon A, Strecker L, Gartner L (1967). Introduction To A Review Of Log Interpretation Methods Used In The Niger Delta. Presented at the SPWLA 8th Annual Logging Symposium, San Antonio, Texas, 12-14 June. SPWLA-1967-Y.
- Ruhovets N, Fertl WH (1982). Volumes, Types, and Distribution of Clay Minerals in Reservoir Rocks Based on Well Logs., paper SPE-10796-MS, SPE Unconventional Gas Recovery Symposium, 16-18 May, Pittsburgh, Pennsylvania, USA.
- Schlumberger (1972). Log Interpretation; Volume 1-Principles Chapt. 16. New York, Texas: Schlumberger.
- Shedid SA (2001). Multi-Purpose Reservoir Characterization Model, paper SPE 68105, the 12th SPE Middle East Oil Show and Conference (MEOS), Manama, Bahrain, March, 17-20.
- Shedid SA, Tiab D, Osisanya S (1998) Improved Reservoir Description of Shaly Sands Using Conventional Well-Log derived Data for Flow Units Identification, Paper SPE 39803, the Permian Basin Oil and Gas Recovery Conference, Texas, USA, March 25-27.
- Shedid-Elgaghah SA, Tiab D and Osisanya S (2001) New Approach for Obtaining J-Function in Clean and Shaly Reservoirs Using In-Situ Measurements. J. Can. Pet. Technol. 40:30-37.
- Simandoux P (1963). Mesures d'electricites en milieu poreux, application a mesure des saturations en eau, Etude du Comportement des massifs Argileux. Supplementary Issue, Revue de l'Institut Francais du Petrol.
- Wylie MRJ, Gregory AR, Gardner LW (1955). Elastic wave velocities in heterogeneous and porous media. Geophysics 21(1):41-70.



Journal of Petroleum and Gas Engineering

Related Journals Published by Academic Journals

- *Journal of Mechanical Engineering Research*
- *Journal of Chemical Engineering and Materials Science*
- *Journal of Engineering and Computer Innovations*
- *Journal of Engineering and Technology Research*
- *Journal of Petroleum Technology and Alternative Fuels*

academicJournals